



HAL
open science

SUC2 sucrose transporter is required for leaf apoplasmic sucrose levels. Consequences for phloem loading strategies

Francoise Vilaine, Laurence Bill, Rozenn Le Hir, Catherine Bellini, Sylvie Dinant

► To cite this version:

Francoise Vilaine, Laurence Bill, Rozenn Le Hir, Catherine Bellini, Sylvie Dinant. SUC2 sucrose transporter is required for leaf apoplasmic sucrose levels. Consequences for phloem loading strategies. 2024. hal-04519245

HAL Id: hal-04519245

<https://hal.science/hal-04519245>

Preprint submitted on 25 Mar 2024

HAL is a multi-disciplinary open access archive for the deposit and dissemination of scientific research documents, whether they are published or not. The documents may come from teaching and research institutions in France or abroad, or from public or private research centers.

L'archive ouverte pluridisciplinaire **HAL**, est destinée au dépôt et à la diffusion de documents scientifiques de niveau recherche, publiés ou non, émanant des établissements d'enseignement et de recherche français ou étrangers, des laboratoires publics ou privés.

1 **SUC2 sucrose transporter is required for leaf apoplasmic sucrose**
2 **levels. Consequences for phloem loading strategies**

3 **Françoise Vilaine ¹, Laurence Bill ¹, Rozenn Le Hir ¹, Catherine Bellini ^{1,2} and Sylvie Dinant ^{1*}**
4

5 **Affiliations :**

6 ¹ Université Paris-Saclay, INRAE, AgroParisTech, Institut Jean-Pierre Bourgin for Plant
7 Sciences (IJPB), 78000, Versailles, France

8 ²Umeå Plant Science Centre, Department of Plant Physiology, Umeå University, 90183
9 Umeå, Sweden
10

11 **Co-authors email addresses:**

12 Françoise Vilaine Francoise.vilaine@inrae.fr

13 Laurence Bill : billlaurence8@gmail.com

14 Rozenn Le Hir rozenn.le-hir@inrae.fr

15 Catherine Bellini catherine.bellini@inrae.fr

16 ***Corresponding author:** Sylvie Dinant: sylvie.dinant@inrae.fr ; Tel.: +33-1-30-83-30-47
17
18

19 **ORCIDs**

20 Françoise Vilaine : [0000-0001-9018-6977](https://orcid.org/0000-0001-9018-6977)

21 Rozenn Le Hir : [0000-0001-6076-5863](https://orcid.org/0000-0001-6076-5863)

22 Catherine Bellini : [0000-0003-2985-6649](https://orcid.org/0000-0003-2985-6649)

23 Sylvie Dinant : [0000-0001-6150-995X](https://orcid.org/0000-0001-6150-995X)
24

25 **Summary statement:** The mechanisms that coordinate apoplasmic and symplasmic loading
26 pathways, and their effects on foliar carbon storage, remain largely unexplored. Surprisingly,
27 the sucrose transporter SUC2 plays a significant role in maintaining sucrose levels in the
28 apoplasm, shedding light on how apoplasmic sugar levels and water flows can interact for
29 phloem loading.
30
31
32
33
34
35
36

37 **Summary**

38 • The SUC/SUT sucrose transporters belong to a family of active H⁺/sucrose symporters,
39 with a role of SUC2 in active apoplastic phloem loading to drive long-distance phloem
40 transport of sucrose in Arabidopsis. However, the cooperation with the symplasmic pathway
41 for phloem loading remains unclear.

42 • In this study, we explored the consequences of reducing either apoplastic or symplasmic
43 pathways of phloem loading. We compared a series of lines with modified expression of *SUC2*
44 gene, and we analyzed the effects on plant growth, sugar accumulation in source and sink
45 organs, phloem transport, and gene expression.

46 • Our data revealed that a modified expression of *SUC2* impacted apoplastic sucrose levels
47 in source leaves but did not impact phloem transport, as might be expected, while increasing
48 foliar storage of carbohydrates. This response differed from lines in which symplasmic
49 communications between phloem cells was disrupted by the over-expression of a
50 plasmodesmata-associated protein, NHL26.

51 • Altogether, our studies indicate an unexpected effect of *SUC2* for apoplastic sucrose
52 levels in source leaves, together with *SUC1*, and suggest a feedback regulation on foliar storage.
53 This data sheds new light on the interplay between symplasmic and apoplastic pathways for
54 sugar loading and the consequences on leaf water flows.

55

56

57 **Key words**

58 Phloem transport; apoplastic; symplasmic ; sugar; water; allocation; partitioning.

59

60

61

62 **Introduction**

63

64 An efficient allocation of photosynthesis products is essential for higher plants to survive as
65 multicellular organisms (Lemoine *et al.*, 2013). The phloem regulates the allocation of sugars in the
66 plant, it controls the entry of sugars into the translocation stream (collection phloem), sugar transport
67 from source to sink organs (transport phloem), and delivery to the various competing sink organs
68 (release phloem) (Van Bel, 2003). In most plants, sucrose is the major transport form. Translocated
69 sucrose provides carbon (C) skeletons for primary metabolism, and supplies energy for cellular
70 metabolism (Nunes-Nesi *et al.*, 2010). It is an essential signaling molecule for cellular metabolic status
71 (Koch, 2004; Li *et al.*, 2021).

72

73 Three loading strategies have been described: active loading from the apoplasm, passive diffusion
74 via the symplasm through plasmodesmata (PD), and passive symplasmic transfer followed by polymer
75 trapping (Rennie & Turgeon, 2009). In apoplasmic loaders, sucrose phloem loading involves a passive
76 efflux of sucrose from leaf bundle sheath or phloem parenchyma cells into the phloem cell wall space
77 through SWEET (SUGAR WILL EVENTUALLY BE EXPORTED) sucrose efflux carriers followed
78 by active, proton-coupled import of sucrose into the companion cells (CC) or the sieve elements (SE)
79 via SUC/SUT (SUCROSE TRANSPORTER) proton-sucrose symporters (Braun, 2022). In
80 Arabidopsis, an apoplasmic loader (Haritatos *et al.*, 2000b), SWEET11/12 are required for the efflux of
81 sucrose in the apoplasm of the phloem parenchyma cells (Chen *et al.*, 2012), and SUC2 is required for
82 its influx into the CC (Gottwald *et al.*, 2000). Their action creates a high sucrose concentration in the
83 CC/SE complex that generates the osmotically driven entry of water, generating the mass flow in the
84 SE. Cell-to-cell transport between mesophyll cells and the perivascular cells and trafficking of sucrose
85 between the CC and the SE in the minor veins, where loading takes place, are symplasmic.
86 Plasmodesmata (PD) opening or closing at the interface between CC and SE can also regulate phloem
87 loading. When the phloem plasmodesmal NDR1/HIN1-like protein NHL26 over-accumulates in the PD,
88 it blocks sugar export in Arabidopsis (Vilaine *et al.*, 2013). Long-distance transport of sugars from
89 sources to sinks is driven by hydrostatic pressure difference. During its transport to the sinks, sucrose is
90 also released and retrieved continuously into the SE (Hafke *et al.*, 2005), its leakage from the SE
91 supplying C to the surrounding tissues (Minchin & Thorpe, 1987). Carbon in excess in the vascular
92 tissues can be stored as starch in the plastids, or as mono or disaccharides in the vacuole, prior to
93 remobilization when sink demand exceeds photosynthetic C supply, as for example during the night.

94

95 The coordination of symplasmic or apoplasmic steps and the mechanisms preventing the flow of
96 sucrose back through PD in various cell types (Turgeon, 2006) remain unclear. Both the apoplasmic and
97 symplasmic pathways may contribute to regulation of the photoassimilate flux (Turgeon & Ayre, 2005;
98 Liesche & Patrick, 2017), depending on species, environmental conditions, and developmental stages.

99 For example, in melon, a symplasmic loader, in response to an infection with the cucumber mosaic virus
100 an increased expression of a gene encoding a SUC/SUT sucrose transporter is observed in source leaves,
101 suggesting that active apoplasmic loading takes over the symplasmic transport (Gil *et al.*, 2011).
102 However, the mechanisms to coordinate apoplasmic and symplasmic loading pathways, and their
103 consequences on foliar C storage, are still unexplored.

104

105 Our previous studies indicated that overexpressing *NHL26* alters sugar allocation in *Arabidopsis*,
106 with higher sugar accumulation in the rosette and impaired phloem sucrose exudation rate (Vilaine *et al.*,
107 2013). We proposed that the phloem loading of sucrose was blocked in over-expressor lines by the
108 reduced permeability of PD at the interface between CC and SE. However, these lines also showed
109 reduced expression of *SUC2*, and this downregulation may also reduced loading. In this study, we
110 intended to explore the consequences of blocking either apoplasmic or symplasmic loading steps on
111 phloem loading by comparing lines impaired in the expression of either *NHL26* or *SUC2*. Our data
112 demonstrate that *SUC2* is required to control the level of sugars in the apoplasm.

113

114 **Materials and Methods**

115

116 *Plant material and growth conditions*

117 The Columbia accession of *Arabidopsis thaliana* (*Col0*) was used in all experiments. The *suc2-4*
118 mutant (SALK_038124) and the partially-complemented line *suc2* x *pGAS:SUC2* (Srivastava *et al.*,
119 2008) were provided by B. Ayre (University of North Texas, USA). The insertional *suc1-3* mutant (Gabi
120 GK139B11) was provided by N. Pourtau (Université de Poitiers, France). It contains a T-DNA insertion
121 in the second intron. The double *suc1 suc2* mutant was obtained by crossing *suc2-4* and *suc1-3*, and
122 homozygous plants were selected with specific primers (Table S1). Plants were grown in soil (Tref
123 Substrates) within a growth chamber under long-days (150 $\mu\text{E m}^{-2} \text{s}^{-1}$, 16 h light 23°C, 8 h darkness
124 18°C, 70% humidity). Plants were fertilized with Plant-Prod nutrient solution (Fertil). In these
125 conditions, the floral bud emerged at 28 days after sowing (DAS) in WT plants. The *suc1suc2* plants
126 were grown under short-days (150 $\mu\text{E m}^{-2} \text{s}^{-1}$, 10 h light 23°C, 14 h darkness 18°C, 70% humidity),
127 based on previous report indicating that *suc2-4* growth and viability are better under such conditions
128 (Srivastava *et al.*, 2009). Projected rosette area (PRA) was measured from pictures and using ImageJ
129 (<https://imagej.nih.gov/ij/>). Rosette and stem growth rates were measured in the linear part of the growth
130 curve between 1-to-4 weeks or 5-to-9 weeks for the rosette and stem growth, respectively, except for
131 *35S:NHL* and *suc2 stems*, measured between 6-to-9 weeks, and 7-to-10 weeks respectively. The harvest
132 index was calculated as the ratio of seed mass to total aerial dry plant mass measured at harvest. For
133 statistics, Student's t test was used, with P values <5. 10^{-2} considered significant. Pearson correlations
134 were realized using R software ('R software, version 3.1.2').

135

136 *Plasmid construction*

137 All constructs were obtained with Gateway technology (Invitrogen). The coding regions of *NHL26*
138 (At5g53730) or *SUC2* (At1g22710) were amplified with specific primers and recombination site-
139 specific sequences. The second step was performed with the primers attB1 and attB2 (Table S2), to
140 reconstitute intact attB recombination sites. PCR fragments were introduced into pDONR207 vector
141 (Invitrogen) by BP recombination and transferred by LR recombination into destination vectors (Table
142 S3). For overexpression driven by the *CmGAS1* promoter from *Cucumis melo*, the destination binary
143 vector pIPK-pGAS-R1R2-tNOS was obtained by inserting a 3083-bp fragment carrying the promoter
144 region *CmGAS1* of galactinol synthase, from the pSG3K101 plasmid, provided by Bryan Ayre
145 (Haritatos *et al.*, 2000a) into the *SpeI* site of pIPKb001 destination vector (Himmelbach *et al.*, 2007).
146 The *amiRNA* to silence *SUC2* gene was designed with WMD3-Web MicroRNA Designer
147 (<http://wmd3.weigelworld.org>) (Ossowski *et al.*) and inserted into the pRS300 vector. The targeted
148 sequence was 5'-CTACTCGTATATGCAGCGTAT-3', corresponding to nucleotide positions 778-798
149 of the *SUC2* ORF, and the *amiRNA* was 5'-TAGATCGCATGACTCAGGCAT-3' (R complement). The
150 *amiRNA* precursor was transferred into pIPK-pGAS-R1R2-tNOS. For plant transformation, binary
151 vectors were introduced into *Agrobacterium tumefaciens* C58pMP90 (Koncz & Schell, 1986) and plants
152 were transformed by floral dip (Clough & Bent, 1998). Transformants were selected on kanamycin (50
153 mg/L) or hygromycin (15 mg/L), depending on binary vector. Homozygous T3 seeds were used for
154 phenotypic analyses.

155

156 *Phloem sap exudates*

157 Phloem sap exudates were collected by EDTA-facilitated exudation (King & Zeevaart, 1974) with
158 modifications. Leaves were sampled 4 h after the beginning of the light period, after floral transition, at
159 first flower opening. Briefly, the petiole of the 5th or 6th rosette leaf was cut off and recut in exudation
160 buffer (10 mM HEPES buffer pH 7.5, 10 mM EDTA), let 5 min in this buffer then transferred in the
161 collection tube with 80 µl of exudation buffer, for 2 hours exudation in the dark. Exudates of six
162 replicates (one leaf per plant and six plants per genotype) were collected. Soluble sugar and amino acid
163 contents were determined on these samples with no purification step. To determine the contaminations
164 due to leakage from cut cells and from the apoplasm, we used the same protocol, excluding EDTA,
165 which prevents the rapid occlusion of sieve tubes, from the exudation buffer (10 mM HEPES buffer pH
166 7.5).

167

168 *Collect of apoplasmic washing fluids (AWF)*

169 AWF were collected using the infiltration-centrifugation method (Lohaus *et al.*, 2001). Plants were
170 grown for 2 months in short-day conditions (150 µE m⁻² s⁻¹, 10 h light 23°C, 14 h darkness 18°C, 70%
171 humidity). Four to six fully developed rosette leaves of six plants were collected, weighed and washed

172 in ice-cold milli-Q water. They were infiltrated with ice-cold milli-Q water containing 0.004% triton
173 X100 by application of a low pressure using a vacuum pump twice for 2 min and wiped dry with tissues,
174 then weighed again. Leaves were then wrapped together, in parafilm and transferred in a syringe (leaf
175 tip pointing downwards). The syringe was placed in a 50 ml Falcon tube and AWF were collected by
176 centrifugation for 20 min at 1000g. The volume of the collected liquid was measured and stored at -
177 20°C for sugar analysis. For *suc2*, the protocol was slightly modified because leaves were smaller and
178 thicker than WT. About 50 leaves were infiltrated for 10 min, wiped dry with tissues, and placed leaf
179 tip down in a 500µL Eppendorf tube in which a hole has been pierced with a needle. The tube was
180 placed in a 1.5ml tube and the AWF was collected by centrifugation for 20 min at 1000g.

181

182 *Soluble sugars, starch, amino acids, total C and N Content.*

183 Leaf carbohydrates and amino acids were analyzed using pooled samples from the 3rd, 4th, 7th and
184 8th rosette leaves collected from the plants utilized for phloem exudate collection. Leaves were
185 harvested 4 h after the onset of the light period and frozen in liquid nitrogen. Soluble sugars and starch
186 were extracted from 50 mg of leaves and quantified using the enzymatic method (Sellami *et al.*, 2019).
187 Amino acids leaf content was determined following the Rosen's method (Rosen, 1957) using the same
188 extracts. Sugars and amino acid contents of phloem exudates and AWF were determined using the same
189 methods, with no hydro-alcoholic extraction. Nitrogen (N) and carbon (C) contents were determined
190 using an elemental analyzer (ThermoFlash 2000; Thermo Scientific).

191

192 *Protein quantification*

193 Seed and leaf proteins were extracted as described (Lu *et al.*, 2020). Two mg of dry seeds or 50 mg
194 of leaf tissue (5th or 6th leaf) were ground in the extraction buffer (100 mM Tris-HCl (pH8), 0.1% [w/v]
195 SDS, 10% [v/v] glycerol] and 2% [v:v] 2-mercaptoethanol). The samples were centrifuged at 14,000g
196 at 4°C for 10 min, and the supernatants were collected. Proteins were quantified using Bio-Rad Protein
197 Assay.

198

199 *Lipid quantification in seeds*

200 Lipid were extracted and quantified from seeds as described (Reiser *et al.*, 2004). First, 0.1 g of air-
201 dried seeds was ground in liquid nitrogen, 1.5 mL isopropanol was added, the resulting extract was
202 transferred into a 1.5-mL reaction tube and incubated with agitation for 12 h at 4°C at 100 rpm.
203 Subsequently, the mixture was centrifuged at 12,000 g for 10 min. The supernatant was transferred into
204 a 1.5-mL tube, then incubated at 60°C overnight to allow the evaporation of isopropanol. Total lipid
205 was quantified gravimetrically.

206

207 *RNA Isolation and Q-RT-PCR*

208 A portion of the leaf material collected for sugar and starch quantification was utilized for RNA
209 extraction. Total RNA was isolated from frozen tissue using TRIZOL (ThermoFisher Scientific).
210 Reverse transcription was conducted with 1 µg total RNA with the Superscript II enzyme (Invitrogen),
211 after DNase treatment (Invitrogen). The primers employed for Q-PCR amplification are listed in Table
212 **S4**. qRT-PCR was carried out with the MESA GREEN MasterMix Plus for SYBR assay, following the
213 manufacturer's instructions (Eurogentec). Amplification was performed with 1 µL of a 1:10 or 1:20
214 dilution of cDNA in a total volume of 10 µL: 5 min at 95°C, followed by 40 cycles of 95°C for 5 s,
215 55°C for 15 s, and 72°C for 40 s, in an Eppendorf Realplex2 MasterCycler (Eppendorf SARL). Two
216 reference genes, *TIP41* (At4g34270) and *APT1* (At1g27450), were utilized, yielding comparable results.
217 The data are presented as percentages of *TIP41* expression. Heat maps were generated after
218 normalization by the mean value of gene expression in WT plants and visualized on Genesis 1.8.1
219 software on a log₂ scale.

220

221 **Results**

222

223 ***Impairing the symplasmic pathway by an over-expression of NHL26***

224

225 The *p35S::NHL26* line (hereafter referred to as *35S:NHL*) carries the coding region of *NHL26*
226 under the 35S promoter (Vilaine *et al.*, 2013) (Fig. **S1a**). The *NHL26* transcript accumulated
227 substantially in *p35S:NHL* lines (300 to 800 times normal levels). We created new transgenic lines in
228 which *NHL26* over-expression was targeted to the CC of the minor veins in mature leaves, using the
229 *CmGAS1* promoter from *Cucumis melo* (Haritatos *et al.*, 2000a) (Fig. **S1a**). These *pCmGAS::NHL26* lines
230 (hereafter called *GAS:NHL*) present an upregulation of *NHL26* (Fig. **S1b,c**) and showed reduced growth
231 and an increased accumulation of soluble sugars in source leaves compared to wild-type plants (Fig.
232 **S1d**).

233

234 Line *GAS:NHL#12*, in which *NHL26* transcript accumulated significantly (100 times normal level)
235 was selected for detailed characterization and comparison with *35S:NHL* line (Fig. **1**). Both lines showed
236 a reduced rosette and stem growth compared to the wild-type, partly due to the delayed flowering in
237 *35S:NHL* line (Fig. **1a-g**), associated with an increased accumulation of soluble sugars and amino acids
238 in the rosette (Fig. **1h,i**). Starch content, bolting time, and harvest index were unchanged in
239 *GAS:NHL#12* plants compared to the wild-type, while they were reduced in *35S:NHL* plants (Fig. **1j-l**).

240

241 Compared to the wild-type, seed protein and lipid contents and 1000-seed-weight were not altered
242 in the *GAS:NHL#12* plants unlike in the *35S:NHL* plants (Fig. **2a-c**). No modification of sugar and starch
243 contents was observed (Fig. **2d,e**). The percentage of N was increased and that of C was reduced in the

244 *35S:NHL* plants (Fig. **2f,g**). This resulted in a significantly reduced C/N ratio in *35S:NHL* seeds (Fig.
245 **2h**). The C/N ratio was also reduced in *GAS:NHL#12* seeds, due to slight -although not significant -
246 variations of seed C and N percentage compared to the wild-type (Fig. **2f,g**). The data indicate that over-
247 expression of *NHL26* in the CC of the minor veins of source leaves reduces plant biomass and increases
248 rosette sugar content. However, the impact is less pronounced compared to what is observed in *35S:NHL*
249 plants.

250

251 Overall, when *NHL26* is overexpressed in minor veins only, i.e. when PD permeability is
252 potentially modified in the collection phloem, the effects observed are milder than when *NHL26* is
253 ubiquitously overexpressed. Although there is no repression of *SUC2* expression in the *GAS:NHL#12*
254 line, unlike in the *35S:NHL* line (Fig. **S1e,f**), the phenotypes can still result from impaired sucrose
255 loading as proposed for *35S:NHL* plants (Vilaine *et al.*, 2013), associated with negative feedback on
256 *SUC2* expression in the minor veins.

257

258

259 ***Impairing the apoplasmic pathway by a reduced expression of SUC2***

260

261 To test the hypothesis that a reduced expression of *SUC2* in the minor veins could affect the
262 overall growth, we analyzed lines in which *SUC2* was either knocked-out (*suc2* mutant), or partially
263 restored in the minor veins of *suc2* mutant (*suc2* x *pGAS:SUC2* line, hereafter referred to as *suc2pC*)
264 (Srivastava *et al.*, 2008), or specifically silenced in the minor veins of source leaves, creating new lines
265 expressing an *amiRNA* targeting *SUC2* and driven by the *CmGAS* promoter (Fig. **S2a**). These lines
266 (hereafter referred to as *miSUC*) have a significantly reduced *SUC2* transcript amount (Fig. **S2b**),
267 associated with a reduced rosette and floral stem growth (Fig. **S2c,d**) and an increased sugar
268 accumulation in source leaves compared with the wild-type (Fig. **S2e**). These phenotypes were more
269 severe as *SUC2* expression decreased (Fig. **S2f**). Two representative lines (*miSUC#4* and #12), *suc2* and
270 *suc2pC* were further characterized (Fig. **3**). A reduction in plant growth was observed at both vegetative
271 and reproductive stages, correlating with the overall decrease in *SUC2* expression (Fig. **3a,b**), while the
272 tissues in which *SUC2* expression is altered are distinct.

273

274 When *SUC2* is knock-out, rosette and stem growth were reduced (Fig. **3c-g**), with a dramatic
275 increase in the accumulation of soluble sugars, amino acids and starch (Fig. **3h-j**) and a delay in
276 flowering and a reduced harvest index (Fig. **3k,l**), consistent with previous reports (Srivastava *et al.*,
277 2008). In *suc2pC*, where *SUC2* expression is restored in minor veins, we observed partial
278 complementation of plant growth (Fig. **3c-g**), associated with less spectacular levels of leaf sugars,
279 amino acids and starch, although they remained high compared to WT (Fig. **3h-j**). In *miSUC#4*,
280 *miSUC#12*, where *SUC2* expression is silenced in minor veins, the growth phenotypes were similar to

281 those of *suc2pC* (Fig. 3c-g), whereas the effects on loading and retrieval are theoretically opposite. By
282 contrast, soluble sugar levels were barely affected in *miSUC#12* with no effect in *miSUC#4* (Fig. 3h),
283 and starch levels were unaffected compared with WT (Fig. 3j). Regarding seed weight and quality,
284 which are severely impaired in *suc2*, we did not observe any complementation of seed weight, protein
285 and lipid content, seed N and C content in the *suc2pC* plants (Fig. 4a-h), although sugar and starch
286 content were unchanged compared with WT (Fig. 4d,e). In contrast, in *miSUC#4*, *miSUC#12*, none of
287 these traits were altered (Fig. 4a-h).

288

289

290 ***Impacts of a modification of SUC2 or NHL26 expression on phloem sugar exudation***

291

292 The reduced growth in the six genotypes compared with the WT, associated with an excess of
293 sugars in the rosette leaves in *GAS:NHL*, *35S:NHL*, *suc2pC* and *suc2* plants, is consistent with an
294 alteration of phloem transport. To test this hypothesis, we collected phloem exudates using EDTA-
295 facilitated exudation method, then measured sucrose and hexoses to calculate sugar exudation rates from
296 cut leaf petioles. In the *35S:NHL* plants, we observed a reduced sucrose exudation rate compared with
297 wild-type plants (Fig. 5a), which is consistent with the initial study of *35S:NHL* lines (Vilaine *et al.*,
298 2013) that concluded that over-accumulation of NHL26 protein leads to the closure PD and blocks sugar
299 loading. The same tendency was observed in the *GAS:NHL* plants, although it was not significant. In
300 *suc2pC* plants, where SUC2 expression is restored in collection phloem, the rate of sucrose exudation
301 was not reduced compared to wild-type plants, consistent with complementation of phloem loading.
302 Surprisingly, when SUC2 was silenced in the minor veins only (*miSUC#4* and *#12* plants), where we
303 expect an impact on phloem loading, the rate of sucrose exudation was not different than that of the
304 wild-type (Fig. 5a). In *suc2* plants, the sucrose exudation rate was dramatically increased compared to
305 wild-type plants with more glucose and fructose in the exudates as well (Fig. S4). The simplest
306 hypothesis to explain the data would be that the increase in sucrose and hexoses results from
307 contamination due to increased leakage from cut petioles.

308

309 In the EDTA-facilitated exudation protocol, EDTA chelates Ca²⁺ ions that would otherwise
310 participate in phloem sealing processes (King & Zeevaart, 1974). The omission of EDTA from the
311 exudation buffer can reveal sugar leakage by a route other than phloem translocation. We measured
312 sucrose in petiole exudates obtained after excluding EDTA from the exudation buffer (Fig. 5b). The
313 data indicate that about 50% of the sugars present in the exudate from *suc2* leaves obtained in the
314 presence of EDTA were also present in exudates without EDTA, revealing high levels of leakage
315 occurring in *suc2* leaves. Such contamination was not observed with the other genotypes, except for the
316 *35S:NHL* plants with more hexose leakage than the wild-type (Fig. S3a).

317

318 To take into account leakage, we corrected the rate of sucrose exudation, by subtracting the leakage
319 values measured in the exudates collected without EDTA from the values of sucrose measured in the
320 exudates collected with EDTA (Fig. 5c). As expected, the corrected exudation rate of sucrose remained
321 reduced in *35S:NHL* plants, which is consistent with earlier report (Vilaine *et al.*, 2013). It was not
322 significantly different in the *GAS:NHL*, *miSUC#4* and *miSUC#12* plants compared to the wild-type.
323 However, it was significantly higher in *suc2* plants (6-fold increase). The corrected values for hexoses
324 were also higher in *suc2* plants than in all other lines (Fig. S3b-e), revealing in *suc2* an increase in the
325 proportions of hexoses in the phloem exudates (Fig. S3f). Interestingly, *SUC2* expression in minor veins
326 of the *suc2* mutant (*suc2pC* plants) totally complemented the wild-type sucrose exudation rate (Fig. 5a;
327 Fig. S4a-c).

328

329

330 ***Impacts of a modification of SUC2 or NHL26 expression on apoplasmic washing fluids (AWF)***

331

332 The data suggested an excess of sugars in the apoplasm. We quantified sugar contents in the AWF
333 collected from rosette leaves. The results revealed elevated sucrose, glucose, and fructose levels in the
334 AWF from *suc2* mutant compared to wild-type plants (Fig. 6a-c). Sugar levels were also higher, albeit
335 to a lesser extent, in the AWF from all the other lines compared to wild-type plants (Fig. 6a-c). Notably,
336 two-fold change was observed in AWF sucrose levels in *GAS:NHL* and *35S:NHL*, about four-fold
337 change in *miSUC#4* and *miSUC#12* and over 20-fold change in the *suc2pC* line. These fold changes
338 observed in the AWF surpassed those noted in the corrected sucrose exudation rates (Fig. S4a). The
339 data indicate that the altered expression of *SUC2* or *NHL26* in either the loading or transport phloem
340 was associated with changes in apoplasmic sugar levels.

341 We also measured amino acid contents in the AWF. The results revealed a modest increase in
342 amino acid levels in the AWF from the *suc2* and *suc2pC* plants, reaching a maximum two-fold change
343 (Fig. 6d) compared to the wild-type. These effects were of a similar magnitude to those observed in
344 corrected phloem exudation rates (2- to 6-fold change compared to the wild-type) (Fig. S4d). The data
345 suggest that the altered expression of *SUC2* or *NHL26* has limited impact on amino acid levels compared
346 to the pronounced effects on sugar levels.

347

348

349 ***Transcriptional responses to impaired phloem sugar loading***

350

351 The important modifications in sugar contents observed in phloem exudates and AWF may lead to
352 defects in sugar homeostasis. We analyzed the expression of a subset of genes (Table S5), coding for

353 sugar transporters and expressed in different leaf tissues (Fig. 7a). It includes genes from the *SUC/SUT*,
354 *SWEET* and *STP* (*SUGAR TRANSPORTER PROTEIN*) families coding for disaccharide and
355 monosaccharide transporters (*SUC1-5*, *SWEET16-17*, *SWEET11-12*, *STP1/13*). It includes genes coding
356 glycolytic enzymes (fructokinases *FRK1, 2, 3, 6, 7*; cell wall invertases *cwINV 1, 3 6*; cytosolic
357 invertases *cINV1-2*, and vacuolar invertases *vINV1-2*), sugar signaling components (hexokinases
358 *HXK1, HXK2*, and trehalose phosphate synthase *TPS5*), and other genes: *GPT2* which encodes the
359 plastidial sugar translocator², *APL3* and *APL4* that encode ADP-Glc pyrophosphorylase large subunits
360 for starch synthesis, *PAP1* which encodes the PRODUCTION OF ANTHOCYANIN PIGMENT1
361 transcription factor and *GSTF12* which encodes a GLUTATHIONE-S TRANSFERASE¹² involved in
362 anthocyanin trafficking. *RRTF1* (REDOX RESPONSIVE TRANSCRIPTION FACTOR 1), *XIP1*
363 (*XYLEM INTERMIXED WITH PHLOEM 1*) and *TRAF-like1* (*TUMOR NECROSIS FACTOR*
364 *RECEPTOR ASSOCIATED FACTOR*), which encodes signaling regulators acting upstream of primary
365 metabolism. Two photosynthesis genes (*LHCB1* and *RBCS*) were also included.

366
367 We observed a higher accumulation of *SUC1*, *SWEET11*, *SWEET12*, *CwINV1*, *CwINV6*, *FRK2*,
368 and *FRK6* transcripts in the lines with modified expression of *SUC2* or *NHL26* compared to wild-type
369 plants (Fig. 7b). A higher transcript amount was observed in the plants showing the highest sugar content
370 for the genes involved in starch biosynthesis (*APL3*, *APL4*, *G6PT2*), glycolysis or sugar signaling
371 (*FRK1*, *FRK5* et *TPS5*), anthocyanin biosynthesis (*GSTF12*, *PAP1*) and *SUC6* and *SUC8* (Fig. 7c-d).
372 Interestingly, the expression of some of these genes was correlated to leaf sucrose content (Table S6).
373 The *SUC3*, *SUC5*, and *SUC9* transcript amounts were either unchanged or slightly reduced in the lines
374 with altered expression of *SUC2* or *NHL26* compared to wild-type plants (Fig. 7e,f). Interestingly, the
375 *SWEET17* (coding tonoplastic facilitator) transcript amount was reduced in the *miSUC*, *suc2pC* and *suc2*
376 plants, unlike *GAS:NHL* and *335S:NHL* plants, in which there was either no change or slight
377 upregulation compared to WT. A similar response was observed for *vINV1* and *vINV2*, coding vacuolar
378 invertases. No variations were observed in the accumulation of *TMT1/TST1* and *TMT2/TST2* transcripts,
379 which code tonoplastic transporters. The *cINV1* and *cINV2* (coding cytosolic invertases) transcript
380 amounts were higher in *GAS:NHL*, *335S:NHL* and *miSUC2* plants, unlike *suc2pC* and *suc2* plants, in
381 which there was no change compared to WT. Finally, the *ERDL6* (coding tonoplastic glucose exporter)
382 transcript amount was higher in *GAS:NHL*, *335S:NHL* and *miSUC2#4* plants compared to WT.

383

384

385 **Additive effects of *suc1* and *suc2* mutations on plant growth**

386

387 There was an upregulation of *SUC1* expression was observed in *NHL* and *SUC* lines, suggesting
388 a potential functional complementation of *SUC2* by *SUC1*. Both *SUC1* and *SUC2* are low-affinity
389 sucrose-transporters with similar sucrose transport activity (Sauer & Stolz, 1994). *SUC1* complements

390 *SUC2* in the *suc2* mutant when expressed from the *SUC2* promoter (Wippel & Sauer, 2012). The
391 function of *SUC1* during the vegetative stage is unclear since *suc1* has a wild-type phenotype for rosette
392 growth (Sivitz *et al.*, 2008). In investigating the possibility of complementation of the *suc2* mutation
393 through the overexpression of *SUC1*, we analyzed the growth phenotype of the *suc1suc2* double mutant
394 (Fig. S5). When grown under short-days, the *suc2* plants exhibited reduced growth compared to *suc1*
395 plants, accompanied by anthocyanin accumulation. Notably, the *suc1suc2* double mutant was smaller
396 than *suc2*, indicating an additive effect with respect to plant growth (Fig. S5).

397
398
399

400 Discussion

401

402 SUC/SUT transporters have been identified in both symplasmic and apoplasmic loaders (Julius
403 *et al.*, 2017). There is a potential for the regulation of those pathways to be coordinated, which could
404 utilize SUC/SUT transporters. In Arabidopsis, which, according to Gamalei's definition (Gamalei,
405 1989), is a type 1-2a apoplasmic loader (Haritatos *et al.*, 2000b), there are PD at the interface between
406 phloem parenchyma cells and companion cells (PPC/CC). SUC2/SUT1 provides influx of sucrose into
407 the CC (Truernit & Sauer, 1995; Stadler & Sauer, 1996). Our current understanding is that SUC2
408 contributes to phloem loading by increasing in the CC/SE complex the osmotic potential that drives
409 water flow into the SE (Gottwald *et al.*, 2000). SUC2 has also been proposed to retrieve the sucrose
410 leaking from the SE back to the transport phloem (Gould *et al.*, 2012). Here, we investigated the
411 possibility of an interplay of *SUC2*-dependent apoplasmic and symplasmic pathways for phloem
412 loading. In *OEX:NHL26* lines, we have postulated that the abnormal buildup of NHL26 at the PDs alters
413 the permeability of PDs between CC and SE (Vilaine *et al.*, 2013), hindering the symplasmic exchange
414 between CC and SE and consequently decreasing phloem loading. Sucrose accumulation in the CC was
415 proposed to trigger negative feedback regulation on the SUC2-dependent sucrose influx, impairing the
416 apoplasmic pathway and phloem loading. In the new series of lines with a modified expression of
417 *NHL26* or *SUC2*, we observed elevated accumulation of sugars, starch, and amino acids in the source
418 leaves, reduced rosette and floral stem growth and reduced seed production. A reduced C/N ratio in the
419 seeds was also observed, revealing reduced carbon and lipid contents. Our findings are consistent with
420 the ¹⁴C labeling studies with *suc2* KO mutants (Gottwald *et al.*, 2000), where carbon allocation from
421 sources to sinks was reduced.

422

423 An unsuspected role for SUC2 and SUC1 in the regulation of sucrose levels in the leaf apoplasm

424

425 Surprisingly, despite the downregulation of *SUC2* expression in the minor veins' CC, the sucrose
426 exudation rate, which serves as a proxy for phloem loading, remains unimpaired in the *miSUC* lines.

427 This suggests that *SUC2* expression in the minor veins' CC may not be essential for maintaining phloem
428 flow. Intriguingly, we observed a concurrent increase in leaf apoplasmic sucrose levels, correlating with
429 the downregulation of *SUC2*. These alterations were also observed in the *suc2pC* line, providing *SUC2*
430 function in the minor veins but defective in *SUC2*-dependent sucrose retrieval in the transport phloem.
431 Our findings suggest that *SUC2* expression in either the collection phloem or the transport phloem
432 affects leaf apoplasmic sucrose levels, and indicate it is not needed to provide phloem mass flow (Fig.
433 **8a-c**).

434

435 The *SUC2* closest ortholog, *SUC1*, has a similar affinity for sucrose (Sauer & Stolz, 1994) and
436 complements *suc2* mutant for sucrose influx (Wippel & Sauer, 2012). The function of *SUC1* in source
437 organs remains unexplored, and there are conflicting reports regarding its expression in leaves. Recent
438 leaf single-cell transcriptomics and translome studies indicate that *SUC1* is expressed in the mesophyll
439 cells (Mustroph *et al.*, 2009; Kim *et al.*, 2021; Xu & Liesche, 2021). In contrast to *SUC2*, which is
440 downregulated by sucrose (Solfanelli *et al.*, 2006), *SUC1* is upregulated (Solfanelli *et al.*, 2006).
441 Consistently, the high sucrose levels in the leaves of *miSUC* and *suc2pC* plants were associated with an
442 increased expression of *SUC1* compared to the wild-type. At the same time, the phloem exudation rate
443 was maintained. Our data suggest that *SUC1* likely functions in the mesophyll cells to retrieve excess
444 sucrose from the apoplasm, similar to its proposed role in the roots (Durand *et al.*, 2018).

445

446 In the two *miSUC* lines, defective for *SUC2* expression in the minor veins, the retrieval of
447 sucrose by *SUC1* may increase cytosolic soluble sugar concentrations in the cells at the periphery of the
448 minor veins while the starch levels remain stable. The downregulation of *HXX1* and *HXX2* and
449 upregulation of *cINVI/2* in *miSUC* plants confirm high sucrose levels in the cytosol. Because phloem
450 transport is maintained in these lines, we propose that the accumulation of sugars may establish a sucrose
451 concentration gradient from the mesophyll to the vascular cells (Fig. **8c**), thereby enhancing diffusion
452 via bulk flow through PD along this gradient, a mechanism proposed for symplasmic loaders (Schulz,
453 2015). Interestingly, in the *suc2pC* line, which lacks *SUC2* expression in the transport phloem – i.e. the
454 main veins - we also observed an upregulation of *SUC1*, with high starch accumulation in the leaf, and
455 upregulation of *G6PT2* and *APL3*, indicating that in this case, high sucrose in the apoplasm also leads
456 to an increased storage capacity for starch. This suggests that the levels of apoplasmic sugars in the
457 transport phloem may also promote starch storage in the plastids.

458

459 These findings support Turgeon's hypothesis (Turgeon, 2010), that active loading evolved not
460 primarily to facilitate phloem transport but to enable plants to utilize foliar carbon reserves.
461 Consequently, both *miSUC* and *suc2pC* lines, despite maintaining a normal phloem sugar exudation
462 rate, accumulated higher levels of non-structural carbohydrates. This accumulation was associated with

463 slower growth rates and reduced rosette and stem growth, consistent with the growth-storage trade-off
464 paradigm (Martínez-Vilalta *et al.*, 2016).

465

466

467 **Apoplasmic sucrose levels and water flows in the phloem.**

468

469 The *suc2* mutant also showed high starch accumulation, reduced rosette and stem growth, high
470 sugar content in leaf AWF, and high *SUC1* expression compared to the wild-type. The data support the
471 hypothesis that excess sucrose in the apoplasm, uptaken by SUC1 in mesophyll cells, creates a cytosolic
472 sucrose concentration gradient, from the mesophyll to the vascular cells (Fig. 8d). We propose that such
473 a gradient facilitates bulk flow diffusion of sucrose through PD, driving symplasmic loading. This
474 hypothesis is supported by the observation that the *suc1suc2* double mutant exhibits an additive
475 phenotype in plant growth (Fig. S5), indicating that sucrose uptake by SUC1 in the mesophyll cells
476 becomes essential in the absence of SUC2 activity, while maintaining phloem loading to some extent.

477

478 Most intriguingly, we observed high sugar amounts in the exudates of the *suc2* plants, revealing
479 dramatic consequences of the loss of *SUC2* expression on phloem transport activity by contrast to the
480 *SUC2* downregulated *miSUC* and *suc2pC* plants. It is reasonable to assume that this is due to a high
481 sugar concentration in the phloem sap. If so, changes in sucrose concentration could contribute to
482 increase phloem sap viscosity and reduce phloem sap flow rate, which has been confirmed
483 experimentally (Gottwald *et al.*, 2000), with a doubling in transit time between organs in *suc2*. This
484 hypothesis is also consistent with earlier ¹⁴C labeling experiments with *suc2*, which demonstrated
485 reduced carbon allocation to the roots (Gottwald *et al.*, 2000) and reduced ¹⁴C level in the exudates
486 (Srivastava *et al.*, 2008). The increase in sucrose concentration might be caused, in part, by the
487 combination of high sugar content in the mesophyll cells, revealed by the high carbohydrate storage in
488 the leaf - and subsequent high symplasmic bulk flow from mesophyll to phloem cells.

489

490 However, the high sucrose concentration in the *suc2* mutant might also result from the reduced
491 entry of water by osmosis in the phloem cells, because of high sucrose concentration in the apoplasm,
492 reducing dramatically phloem mass flow, which is driven by an osmotically generated pressure gradient
493 between the apoplasm and the cytosol. We showed a high sugar concentration in the AWF of *suc2*,
494 which may minimize the osmotic potential difference across the plasma membrane of the PPC and
495 CC/SE complex, thereby limiting water uptake. A reduced radial water flow potentially leads to elevated
496 sucrose concentration in the sap and increased viscosity, reducing phloem flow rate. We propose that a
497 combination of low flow velocity and high sap viscosity increases the turgor pressure of the SE in *suc2*
498 (Fig. 8d), explaining the very high rates of sucrose exudation in *suc2* after sectioning the highly
499 pressurized sieve tubes.

500

501 Our findings provide new insights into the *suc2* mutant phenotype. Gould et al. (Gould *et al.*,
502 2012) suggested that the absence of SUC2 in the collecting phloem reduces turgor pressure in SE and
503 slowing down transport. However, the elevated sugar exudate rates and sugar levels in the apoplasmic
504 fluids of *suc2* contradict Gould's hypotheses, suggesting high osmotic potentials in both compartments.
505 Contrary to Gould's proposals, our findings imply that *SUC2 loss of function*-mediated elevation of
506 apoplasmic sucrose content in the phloem impedes the water flow that drives phloem flow.

507

508

509 **Sap viscosity, turgor pressures and phloem unloading.**

510

511 Another feature of *suc2* plants was a reduction in seed weight and lower C, protein and lipid
512 contents in the seeds, effects that were also observed in *suc2pC* plants, compared to the wild-type, which
513 suggests an impairment in phloem unloading in sink organs. Interestingly, as observed in young
514 seedlings *in vitro* (Gottwald *et al.*, 2000), *suc2* root growth is severely reduced compared to wild-type,
515 which is partially mitigated in a sugar-rich environment (Fig. **S6**). Unloading of solutes in the root is
516 mainly symplasmic, through funnel-PD at the root tip, driven by a combination of mass-flow and
517 diffusion through PD (Ross-Elliott *et al.*, 2017). Our findings of high sugar in the AWF and high rate of
518 sugar exudation suggest high sap viscosity in the sieve tubes and a high turgor pressure. Interestingly,
519 as observed in young seedlings *in vitro* (Gottwald *et al.*, 2000), root growth is partially mitigated in a
520 sugar-rich environment (Fig. **S6**). Several studies have shown that the PD permeability is osmo-
521 regulated in response to turgor pressure exerted on both sides of the PD (Hernández-Hernández *et al.*,
522 2020). When osmolyte concentrations, such as sucrose, become excessively high on one side,
523 plasmodesmata close, disrupting symplasmic connectivity. Our findings indicated that in a hypertonic
524 sugar-rich environment, there may be less disparity in the osmotic potential of the root outer cell layers
525 and in phloem cells. Consequently, a hypertonic environment should restore PD connectivity and
526 facilitate symplasmic unloading at the root tip, potentially accounting for the observed increase in root
527 growth in a sugar-rich environment.

528

529

530 **Impacts of apoplasmic and symplasmic loading strategies on foliar carbon storage**

531 The significant increase in sucrose content observed in the AWF of the *NHL* and *SUC* lines
532 compared to the wild-type was associated with an increased expression of *cwINV1* and *SUC1*, two genes
533 expressed in mesophyll cells (Kim *et al.*, 2021; Xu & Liesche, 2021) and with elevated foliar soluble
534 sugars. These results suggest that even minor reductions in symplasmic or apoplasmic pathways increase
535 foliar carbon storage in the mesophyll. Correspondingly, genes involved in photosynthesis (e.g., *RBCS*

536 and *LHCBI*) or cytosolic glucose signaling (e.g., *HXK1* and *HXK2*) exhibited slight downregulation in
537 some lines, aligning with negative feedback regulation of photosynthesis by high sugar levels (Griffiths
538 *et al.*, 2016). The data highlight shared metabolic and photosynthetic responses to impaired *SUC2*-
539 dependent apoplasmic or impaired symplasmic sugar loading. Additional genes like *FRK2*, *FRK6*,
540 *SWEET11*, and *SWEET12*, expressed in phloem cells, are consistently upregulated across all lines,
541 suggesting a subsequent impact on the pools of cytosolic soluble sugar in vascular tissues.

542 We observed marked differences in the foliar carbon storage of the plants impaired in the
543 symplasmic pathway, *35S:NHL* and *GAS:NHL*, with a moderate soluble sugar accumulation compared
544 to the plants impaired in the *SUC2*-apoplasmic pathway. Remarkably, it was also associated with a
545 reduction in the sucrose exudation rate in *35S:NHL* plants, with a similar trend observed in *GAS:NHL*
546 *plants*, in contrast to no alteration in exudate rates in *miSUC* and *suc2pC* plants. This finding rules out
547 the hypothesis that the reduction was due to impaired *SUC2*-mediated apoplasmic phloem loading,
548 which maintained the sucrose exudation rate. Instead, we propose that PD-dependent sucrose transport
549 between the CC and the SE is also disrupted in the *GAS:NHL* line (Fig. **8e,f**), thus reducing phloem
550 loading.

551 Interestingly, the foliar accumulation of soluble sugars in *GAS:NHL* and *35S:NHL* plants
552 correlates with the up-regulation of *vINV1* and/or *vINV2*, key players in vacuolar sucrose turnover
553 required for proper plant development (Vu *et al.*, 2020). This suggests that the symplasmic pathway
554 influences sucrose homeostasis within the vacuole. In contrast, in lines with impaired *SUC2* expression
555 the observation of a downregulation of *vINV1*, *vINV2*, and *SWEET17* implies distinct
556 consequences for sugar partitioning when apoplasmic pathway is impaired. However, the active
557 tonoplasmic sugar transporter genes *TMT1/2* remained unaffected, indicating a complex interplay in
558 sugar partitioning between the apoplasm and the vacuole — an aspect that has been inadequately
559 explored thus far. Based on these observations, we propose that the symplasmic and *SUC2*-dependent
560 apoplasmic pathways differentially impact foliar carbon storage, favoring either sugar storage in the
561 vacuole or starch in the chloroplasts, depending on apoplasmic sugar levels and water flows.

562 563 **Conclusions** 564

565 Our findings confirm the pivotal role of *SUC2* in regulating phloem loading and unloading. The
566 data support the hypothesis that *SUC2* achieves this by affecting sucrose levels in the apoplasm, thereby
567 influencing water potential gradients and impacting water flow into or out of the phloem cells.
568 Moreover, the data suggest that differences in osmotic potential between the apoplasm and the cytosol,

569 responsible for water entry in the CC/SE complex, may alter phloem loading. This, in turn, may affect
570 the permeability of PD for unloading, as suggested by Yan & Liu (Yan & Liu, 2020).

571 The suggested collaborative role of *SUC2*, working alongside *SUC1* to regulate sugar content
572 in the apoplasm and to control water flow to the phloem, could have significant implications for leaf
573 water status and photosynthesis. It has long been recognized that sugar levels in the apoplasm, including
574 sucrose and glucose, influence guard cell regulation, stomatal opening, and gas exchanges (Daloso *et*
575 *al.*, 2016; Flütsch & Santelia, 2021). Whether the activity of *SUC1/SUC2* in apoplasmic sugar regulation
576 contributes to the negative feedback regulation of sugars on photosynthesis remains a subject for future
577 investigation.

578

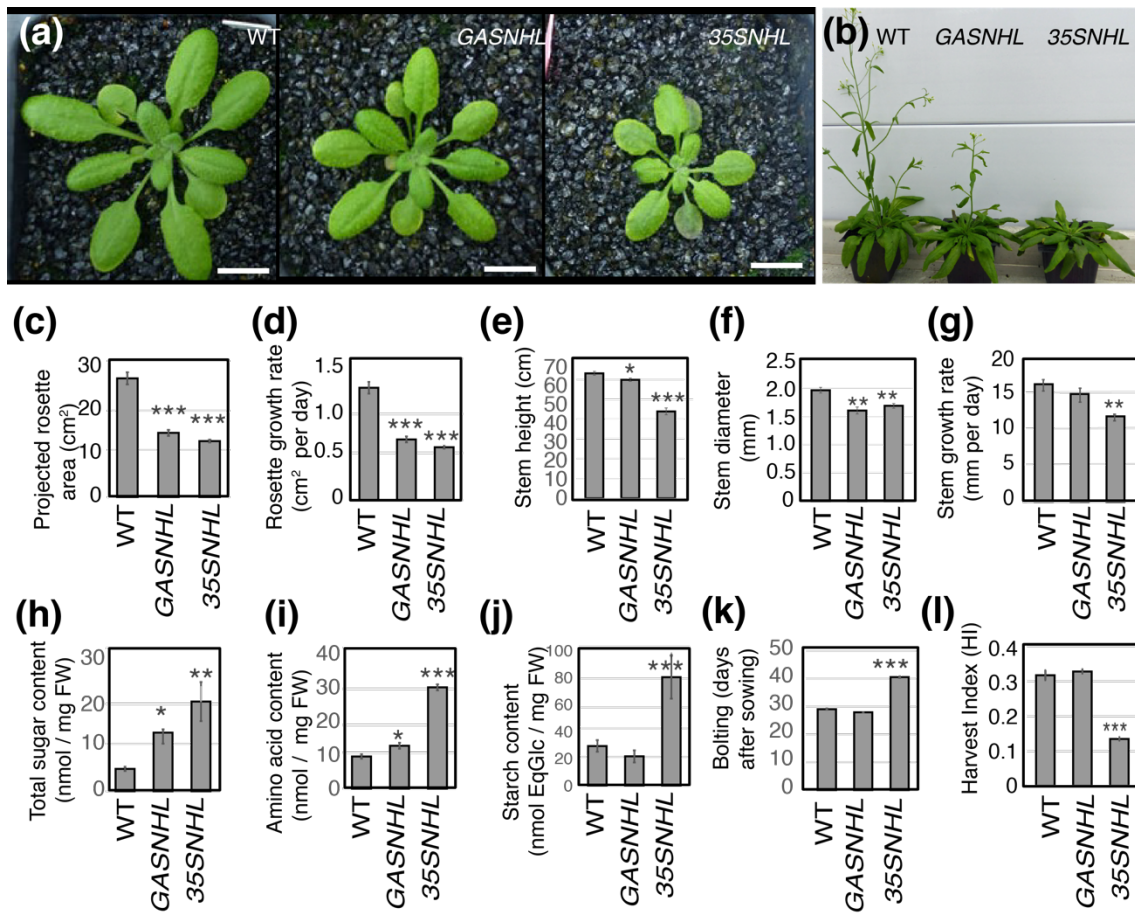
579 **Acknowledgments:** We thank Hervé Ferry and Joël Talbotec for taking care of the plants in the greenhouse
580 facility. We thank Roua Jeridi for her help to the initial collects of apoplasmic washing fluids. We thank the Plant
581 Observatory. This work has benefited from the support of IJPB's Plant Observatory technological platforms. The
582 IJPB benefits from the support of Saclay Plant Sciences-SPS (ANR-17-EUR-0007). We thank Dr Michael Thorpe
583 for his helpful comments that improved the manuscript. We thank Bryan Ayre and Nathalie Pourtau for the gift of
584 seeds and plasmids.

585
586 **Conflicts of interest :** The authors declare that the research was conducted in the absence of any
587 commercial or financial relationships that could be construed as a potential conflict of interest.

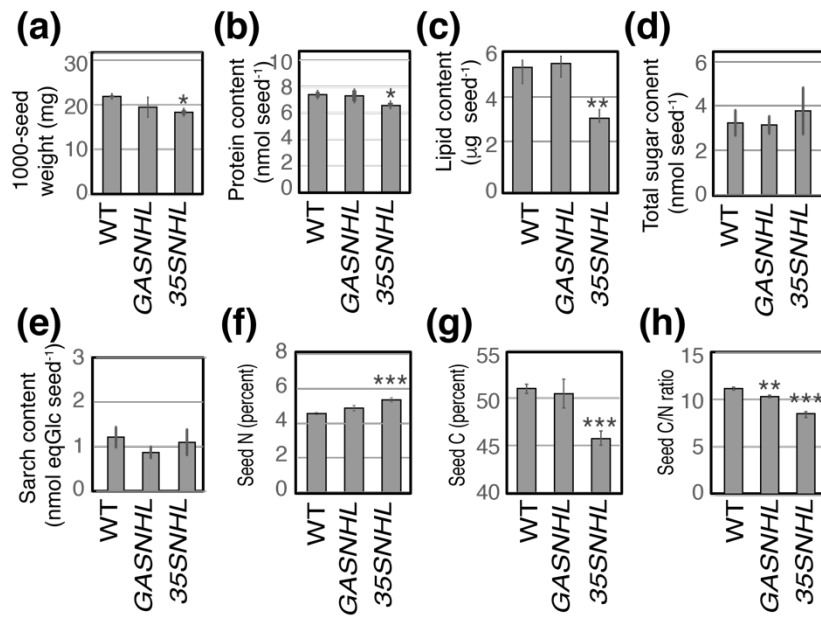
588
589 **Author Contributions:** F.V. and S.D. conceived and supervised the experiments. F.V. and L.B.
590 realized the experiments. First draft was done by S.D. Editing was done by S.D., F.V., R.L.H. and C.B.

591
592 **Data availability :** Raw data and seeds from Arabidopsis lines supporting the findings of this study
593 are available from the corresponding author SD on request.

594
595 **Funding:** Preliminary studies realized in this work benefited from the support of the BAP
596 department of INRAE (Vasculodrome's project). The IJPB benefits from the support of the LabEx
597 Saclay Plant Sciences-SPS (ANR-17-EUR-0007). This work benefited from the support of IJPB's Plant
598 Observatory technological platforms.

603 **Fig. 1 Phenotype of the *GAS:NHL* and *35S:NHL* plants**

604 **(a):** Phenotype of 3 weeks-old plants. **(b):** Phenotype of 6 weeks-old plants. **(c):** Projected rosette area
 605 (PRA) of 4 weeks-old plants (cm²). **(d):** Rosette growth rate between 7 and 21 days after sowing (DAS)
 606 (cm² per day). **(e):** Floral stem height of 10 weeks-old plants (cm). **(f):** Floral stem diameter of 10 weeks-
 607 old plants (mm). **(g):** Floral stem growth rate between 35 and 56 DAS (mm per day). **(h):** Total soluble
 608 sugar content (sucrose, glucose and fructose) in nmoles per mg of fresh weight (FW) in rosette leaves.
 609 **(i):** Total amino acids content in nmoles per mg of FW in rosette leaves. **(j):** Starch content in nmoles
 610 EqGlucose per mg of FW in rosette leaves. **(k):** Bolting time (DAS). **(l):** Harvest index (HI). Bar plots
 611 and error bars represent the mean and *se* (*n* = 6). Asterisks indicate significant differences compared to
 612 control plants (* *p* < 0.05; ** *p* < 0.01; *** *p* < 0.001).

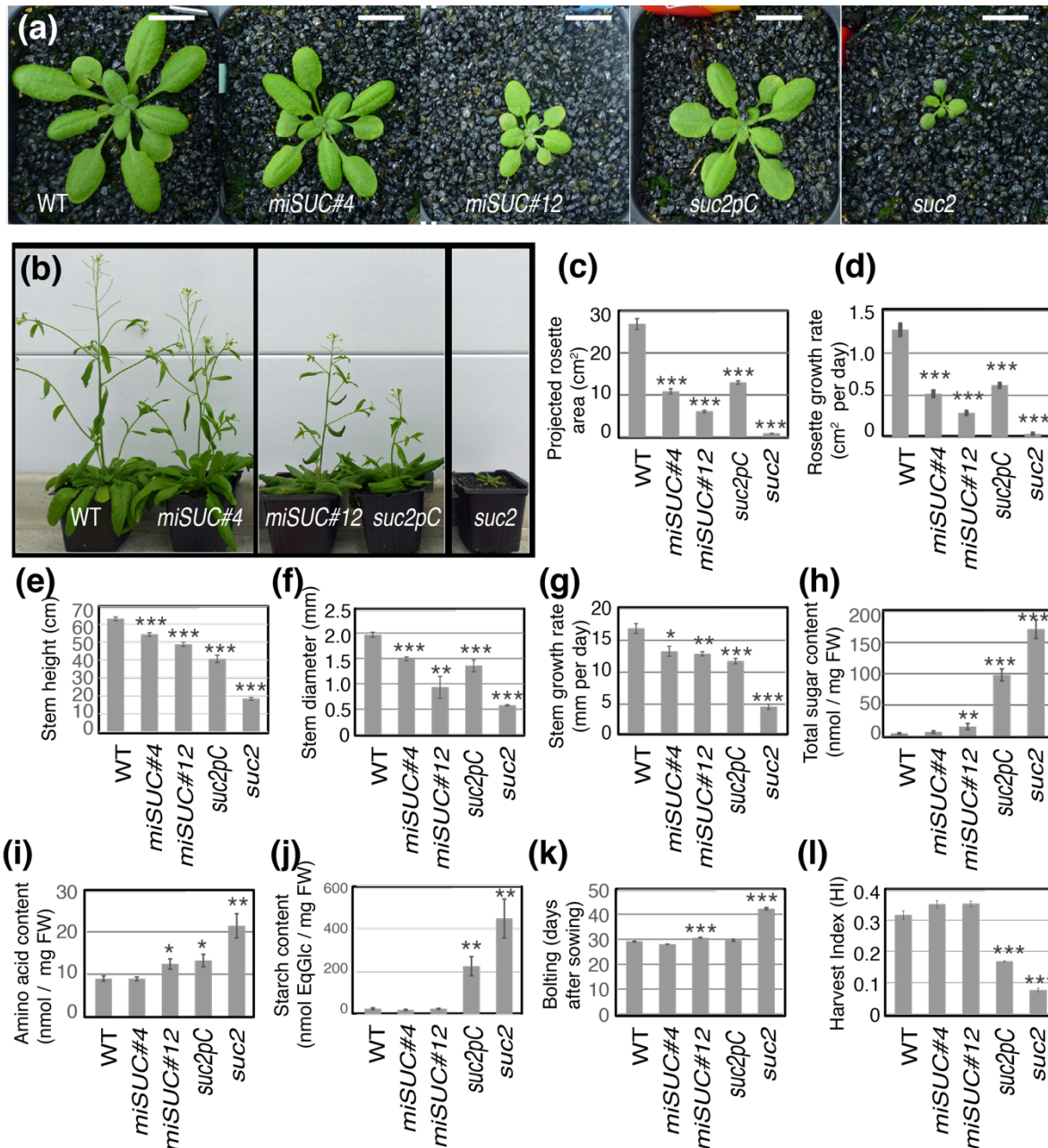


614
615

616 **Fig. 2 Seed phenotype of the *GAS:NHL* and *35S:NHL* plants.**

617 **(a):** Weight of 1000-seeds (mg). **(b):** Protein content (nmoles/seed). **(c):** Lipid content (µg/seed). **(d):**
618 Total sugar content (sucrose, glucose and fructose) (nmoles/seed). **(e):** Starch content (nmoles
619 EqGlucose /seed). **(f):** Percentage of N in seeds. **(g):** Percentage of C in the seeds. **(h):** C/N ratio in
620 seeds. Bar plots and error bars represent the mean and *se* (*n* = 6). Asterisks indicate significant
621 differences compared to control plants (* *p* < 0.05; ** *p* < 0.01; *** *p* < 0.001).

622



623

624

Fig. 3 Phenotype of the *SUC* lines

625

(a): Phenotype of 3 weeks-old plants. **(b):** Phenotype of 6 weeks-old plants. **(c):** Projected rosette

626

area (PRA) of 4 weeks-old plants (cm²). **(d):** Rosette growth rate between 7 and 21 days after sowing

627

(DAS) (cm² per day). **(e):** Floral stem height of 10 weeks-old plants (cm). **(f):** Floral stem diameter of

628

10 weeks-old plants (mm). **(g):** Floral stem growth rate between 35 and 56 DAS (mm per day). **(h):**

629

Total soluble sugar content (sucrose, glucose and fructose) in nmoles per meg of fresh weight (FW) in

630

rosette leaves. **(i):** Total amino acids content in nmoles per mg of FW in rosette leaves. **(j):** Starch

631

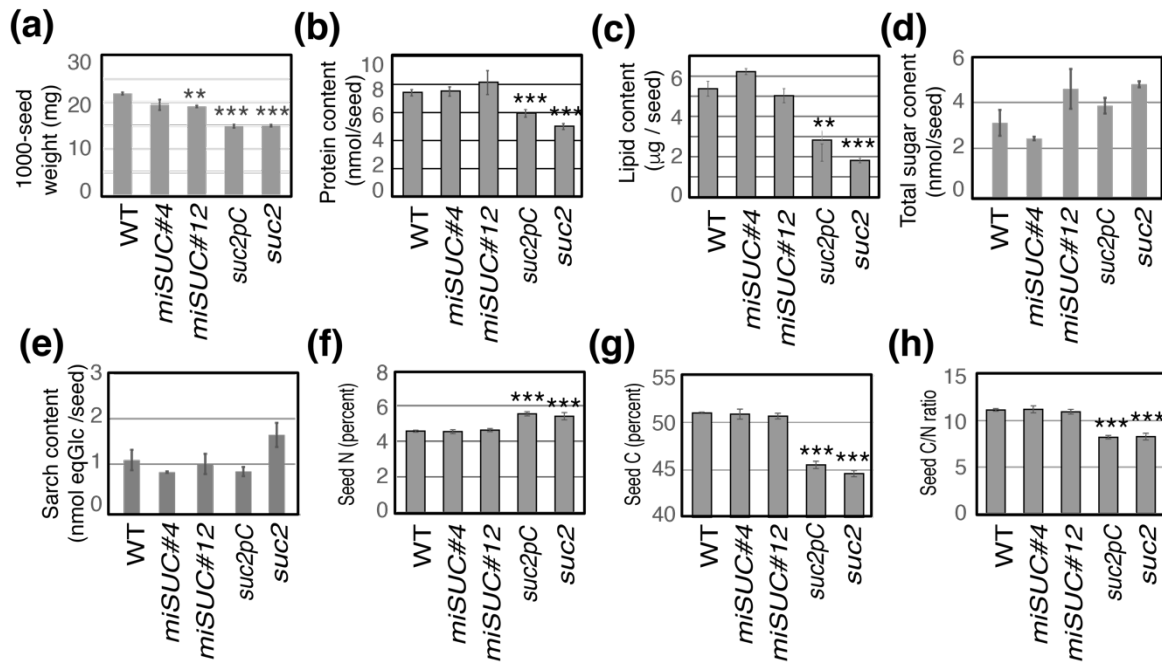
content in nmoles EqGlucose per mg of FW in rosette leaves. **(k):** Bolting time (in days). **(l):** Harvest

632

Index (HI). Bar plots and error bars represent the mean and *se* (*n* = 6). Asterisks indicate significant

633

differences compared to control plants (* *p* < 0.05; ** *p* < 0.01; *** *p* < 0.001)

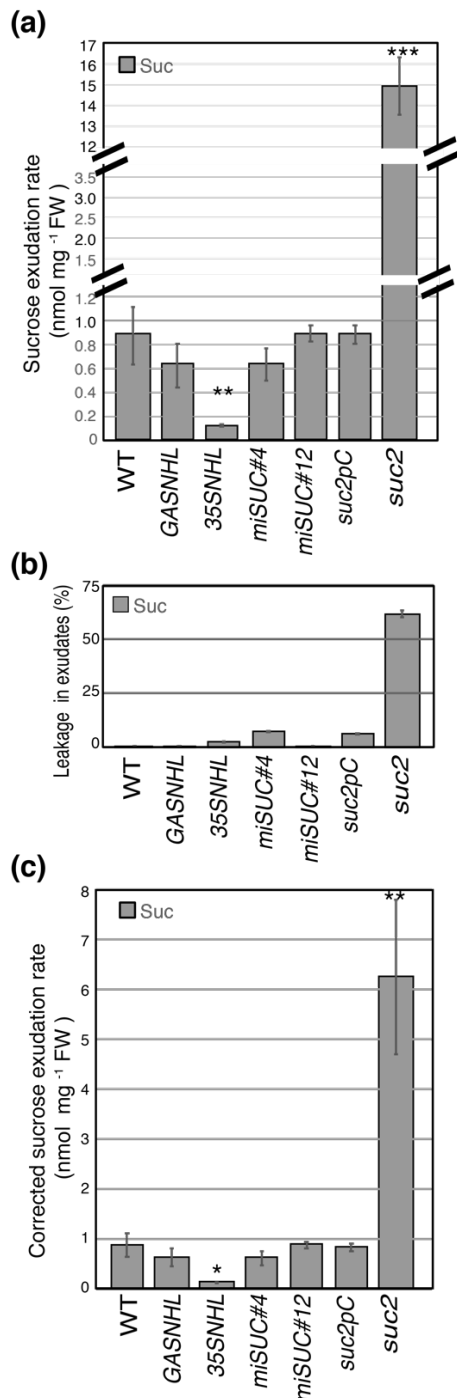


634

635 **Fig. 4 Seed phenotype of the *SUC* lines**

636 (a): Weight of 1000-seeds (mg). (b): Protein content (nmole/seed). (c): Lipid content (µg/seed). (d):
 637 Total sugar content (sucrose, glucose and fructose) (nmole/seed). (e): Starch content (nmol EqGlucose
 638 /seed). (f): Percentage of N in seeds. (g): Percentage of C in the seeds. (h): C/N ratio in seeds. Bar plots
 639 and error bars represent the mean and *se* (*n* = 6). Asterisks indicate significant differences compared to
 640 control plants (* *p* < 0.05; ** *p* < 0.01; *** *p* < 0.001).

641



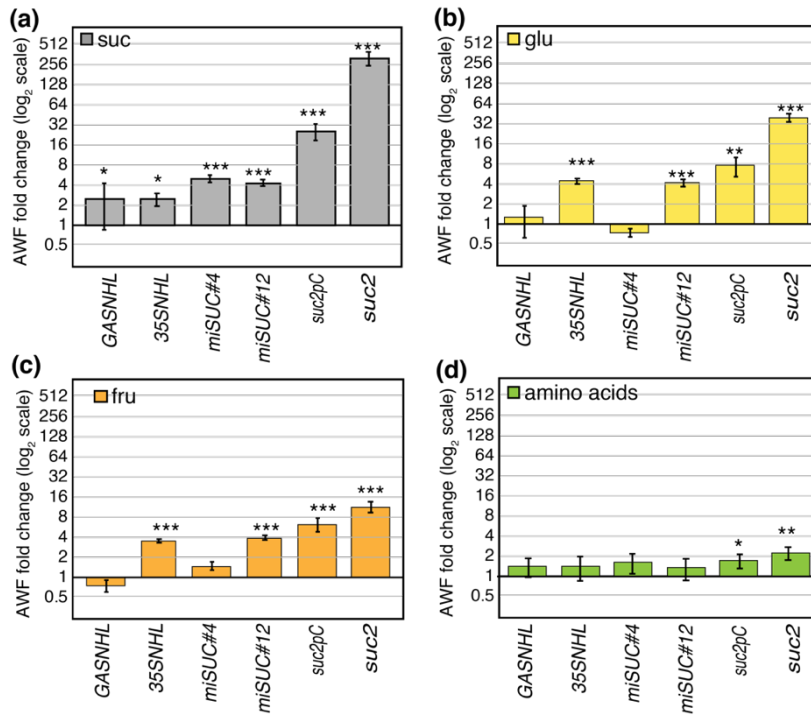
642

643 **Fig. 5 Rate of phloem sucrose exudation in NHL and SUC plants**

644 **(a):** Sucrose exudation rate was measured on the phloem exudate collected by EDTA-facilitated
 645 exudation of one rosette leaf per plant (5th or 6th leaf) for 2 hours of exudation. **(b):** Sucrose leakage was
 646 measured on the exudate on a second rosette leaf of the same plant (5th or 6th leaf) collected using the
 647 same method but omitting EDTA. **(c):** Corrected exudation rate of sucrose, calculated by subtracting
 648 sucrose leakage value from the exudation rate. Bar plots and error bars represent the mean and *se* (*n* =
 649 6). Asterisks indicate significant differences compared to control plants (* *p* < 0.05; ** *p* < 0.01; *** *p*
 650 < 0.001). FW: fresh weight.

651

652



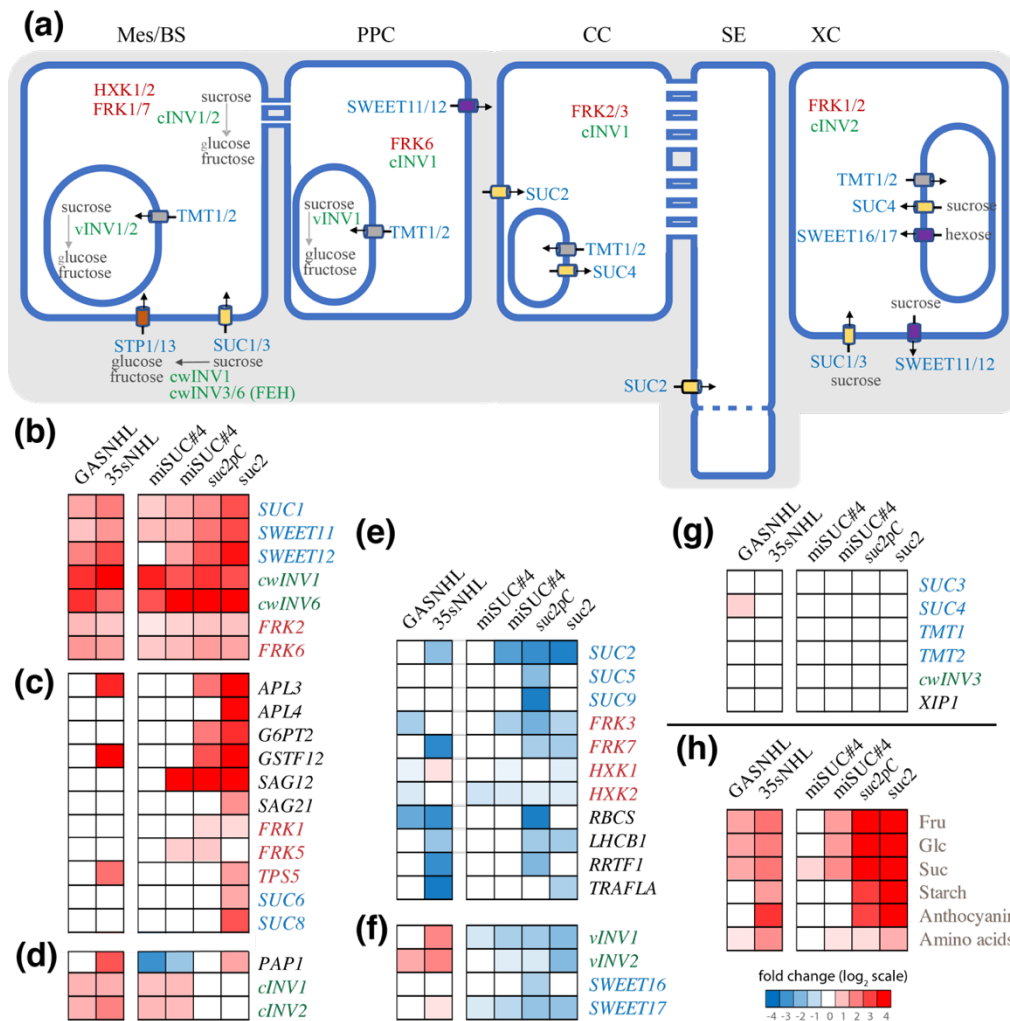
653

654 **Fig. 6 Sugars and amino acids in the apoplasmic washing fluids in NHL and SUC2 plants**

655 (a) Sucrose, (b) glucose, (c) fructose and (d) amino acids contents (measured in nmoles per mg of fresh

656 weight) in the leaf apoplasmic washing fluids (AWF), and expressed as fold change compared to WT.

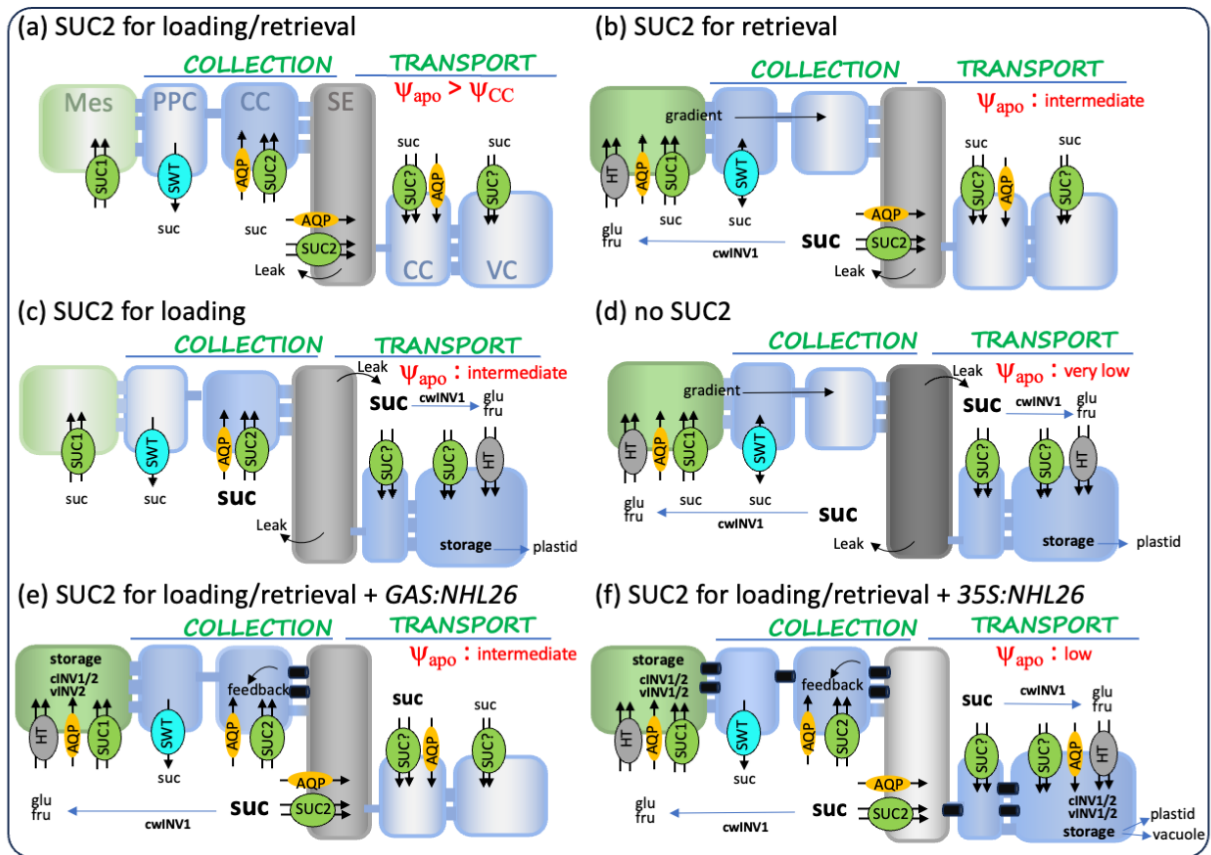
657



658

659 **Fig. 7 Fold change in transcript amounts in NHL and SUC plants**

660 (a): Cell type specific expression of the selected genes (modified from Xu & Liesche 2021) (Xu &
 661 Liesche, 2021). In blue letters: genes coding sugar transporters, in green, genes coding invertases, in
 662 red, genes coding FRK, HXK or TPS. In black miscellaneous. Mes: mesophyll, BS: bundle sheat, PPC:
 663 phloem parnehcyoma cells, CC: companion cells, SE: sieve elements, XC: xylem cells. (b) to (g): Heat
 664 map showing fold changes in relative transcript amount for selected genes in the NHL and SUC lines
 665 compared to WT. (b) (c) and (d): genes showing an upregulation in NHL and/or SUC lines. (e): genes
 666 showing a downregulation in NHL and/or SUC lines. (f): genes showing opposite response in NHL or
 667 SUC2 lines. (g) genes showing no significant changes in NHL and SUC lines. (h) Heat map showing
 668 fold changes in soluble sugars, starch, anthocyanins and amino acids content in rosetted. Fold change
 669 are shown in a log₂ scale, with blue indicating significant lower values in NHL or SUC lines compared
 670 to WT, and in red indicating higher values ($p < 0.05$, $n = 4-6$).



671
 672
 673
 674
 675
 676
 677
 678
 679
 680
 681
 682
 683
 684
 685
 686
 687
 688
 689

Fig. 8 Proposed model of the roles of SUC1 and SUC2 in regulating apoplasmic sucrose levels, phloem loading and carbohydrate storage in various genotypes.

Phloem apoplasmic and symplasmic pathways are shown, for our genotypes. Passive diffusion of sucrose occurs through plasmodesmata (PD) and water exchange across membranes are facilitated by aquaporins (AQP). In the COLLECT phloem, intercellular transport of sucrose is typically mediated by efflux from PPC (phloem parenchyma cells) *via* to SWEET facilitators, followed by influx in CCto (companion cells) or SE (sieve elements) *via* the SUC2 active sucrose/proton symporter, or into Mes (mesophyll cells) *via* SUC1. Sucrose can also be cleaved by invertases (INV) into hexoses with influx by hexose transporters (HT). In the TRANSPORT phloem, sucrose that has leaked from the SE can be retrieved by SUC2 into the SE or stored in vascular cells (VS) after influx mediated by unidentified sucrose (SUC) or hexose transporters (HT). In this model, AQP are only indicated in cells where the apoplasmic water potential is higher than that of the cytosol and causes entry of water. *SUC2*, specifically expressed in the CC, is downregulated in response to high leaf sucrose levels, while *SUC1*, expressed in the mesophyll, is upregulated under the same conditions.

690 **(a):** In wild-type plants, loading results from efflux of sucrose into the apoplasm of the phloem
691 parenchyma cells by SWEET 11 and SWEET12, its entry into the CC by SUC2, then passive
692 diffusion through PD between CC and SE. Under normal conditions, SUC2 regulates the
693 sucrose concentration in the apoplasm of the CC/SE complex, thereby maintaining a water
694 potential difference across the plasma membrane of the CC/SE. This enables water uptake into
695 the CC and the SE in the collection phloem, generating axial phloem mass flow. It also supports
696 water uptake in the transport phloem in coordination with sugar retrieval along the transport
697 pathway, limiting the storage of sugars in the VC.

698

699 **(b):** When SUC2 is inactive in the collection phloem, as in *miSUC* lines, increased sucrose
700 concentration occurs in the apoplasm of the minor veins. This perturbation impacts the water
701 potential and impairs water uptake in the SE/CC complex. The high levels of sucrose in the
702 apoplasm, in turn, induce the upregulation of *SUC1*, increasing the sucrose influx in mesophyll
703 cells and creating a gradient of sucrose concentration from the mesophyll to the phloem. This
704 process shifts the phloem loading towards a symplasmic pathway, which maintains the phloem
705 mass flow.

706

707 **(c):** When SUC2 is inactive in the transport phloem, as in *suc2pC* line, increased sucrose
708 concentration occurs in the apoplasm of the CC and VC. This likely reduces water uptake in
709 these cells, and carbohydrates in excess are preferentially stored as starch in the plastids.

710

711 **(d):** When *SUC2* is inactive in the collection and in the transport phloem, as observed in the
712 *suc2* mutant, a dramatic increase in sucrose concentration occurs in the apoplasm of the phloem
713 cells, which lowers apoplasmic water potentials and prevents the entry of water in phloem cells.
714 The subsequent upregulation of *SUC1* in the mesophyll cells, increases sucrose influx in the
715 mesophyll cells, and shifts the phloem loading towards a symplasmic pathway. However, the
716 low osmotic potential in the apoplasm poses a challenge by restricting water entry across the
717 plasma membranes of phloem cells. This limitation impacts phloem mass flow, both reducing
718 phloem sap velocity and increasing sap viscosity. Carbohydrates in excess are stored as starch
719 in the plastids.

720

721 **(e):** When SUC2 is active, the increased *NHL26* expression in the minor veins in the *GAS:NHL*
722 line, impacts PD permeability, elevating sucrose levels in CC cytosol within the collection
723 phloem. This reduces *SUC2* expression through a feedback mechanism, increasing sucrose

724 concentrations in the apoplasm. However, the osmotic effect is insufficient to impede water
725 entry in the minor veins, thereby maintaining the phloem mass flow. However, the high
726 apoplasmic sucrose levels cause an upregulation of *SUC1*, increasing sucrose influx in the
727 mesophyll cells and promoting an accumulation of soluble sugars in those cells, notably in the
728 vacuole.

729

730 **(f)**: When *SUC2* is active, the overexpression of *NHL26* in *35S:NHL* line, alters plasmodesmata
731 permeability, elevating sucrose levels in CC cytosol within the collection and transport phloem.
732 This negatively affects *SUC2* expression and increases sucrose concentrations in the apoplasm.
733 A low water potential in the apoplasm likely impedes water entry in the minor veins, resulting
734 in reduced phloem mass flow. The excess sucrose accumulates in the phloem parenchyma cells
735 and in mesophyll cells, where it is stored, as starch in the plastids and soluble sugars in the
736 vacuole.

737

738 Mes: Mesophyll cell, PPC: phloem parenchyma cell, CC: companion cell, SE: sieve element,
739 VC: vascular cell. Phloem cells are in blue (CC, PPC and VC) and grey (SE), and mesophyll
740 cells in green (Mes). The intensity of the color (blue, green or grey) represents the levels of
741 sucrose in the cell, with a light color corresponding to a low level and an intense color to a high
742 level. SUC: sucrose transporter, HT= hexose transporter, SWT: SWEET11/12 facilitator,
743 AQP=aquaporin, cwINV= cell wall invertase, cINV=cytosolic invertase, vINV=vacuolar
744 invertase. Open plasmodesmata are represented in blue, closed plasmodesmata occluded by
745 *NHL26* in black. Ψ_{apo} : water potential of the apoplasm.

746

747 **Supporting Information**

748

749 Fig. S1. Characterization of the *NHL*- lines.

750 Fig. S2. Characterization of the *SUC*- lines.

751 Fig. S3. Rate of phloem hexoses and amino acids exudation in *NHL*- and *SUC*- lines.

752 Fig. S4. Fold-changes compared to WT of corrected exudation rates of sugars and amino acids in *NHL*-
753 and *SUC*- lines.

754 Fig. S5. Phenotype of the *suc1* and *suc2* simple and double mutants.

755 Fig. S6. *In vitro* root growth of WT and *suc2* seedlings.

756 Table S1. Primers for genotyping.

757 Table S2. Primers for Gateway^R cloning

758 Table S3. Vectors for cloning.

759 Table S4. Primers for quantifying genes by RT-qPCR.

760 Table S5. List of genes analyzed by RT-qPCR

761 Table S6. Correlations (R_{pearson}) between gene expression and sugar accumulation in rosette leaves.

762

763 **References**

764

765 **Van Bel AJE. 2003.** The phloem, a miracle of ingenuity. *Plant, Cell & Environment* **26**: 125–149.

766 **Braun DM. 2022.** Phloem loading and unloading of sucrose: what a long, strange trip from source to sink.

767 *Annual Review of Plant Biology* **73**: 1–32.

768 **Chen L-Q, Qu X-Q, Hou B-H, Sosso D, Osorio S, Fernie AR, Frommer WB. 2012.** Sucrose efflux mediated
769 by SWEET proteins as a key step for phloem transport. *Science* **335**: 207–211.

770 **Clough SJ, Bent AF. 1998.** Floral dip: A simplified method for *Agrobacterium*-mediated transformation of
771 *Arabidopsis thaliana*. *Plant Journal* **16**: 735–743.

772 **Daloso DM, dos Anjos L, Fernie AR. 2016.** Roles of sucrose in guard cell regulation. *New Phytologist* **211**:
773 809–818.

774 **Durand M, Mainson D, Porcheron B, Maurousset L, Lemoine R, Pourtau N. 2018.** Carbon source–sink
775 relationship in *Arabidopsis thaliana*: the role of sucrose transporters. *Planta* **247**: 587–611.

776 **Flütsch S, Santelia D. 2021.** Mesophyll-derived sugars are positive regulators of light-driven stomatal opening.
777 *New Phytologist* **230**: 1754–1760.

778 **Gamalei Y. 1989.** Structure and function of leaf minor veins in trees and herbs - A taxonomic review. *Trees* **3**:
779 96–110.

780 **Gil L, Yaron I, Shalitin D, Sauer N, Turgeon R, Wolf S. 2011.** Sucrose transporter plays a role in phloem
781 loading in CMV-infected melon plants that are defined as symplastic loaders. *Plant Journal* **66**: 366–374.

782 **Gottwald JR, Krysan PJ, Young JC, Evert RF, Sussman MR. 2000.** Genetic evidence for the *in planta* role
783 of phloem-specific plasma membrane sucrose transporters. *Proceedings of the National Academy of Sciences* **97**:
784 13979–13984.

785 **Gould N, Thorpe MR, Pritchard J, Christeller JT, Williams LE, Roeb G, Schurr U, Minchin PEH. 2012.**
786 AtSUC2 has a role for sucrose retrieval along the phloem pathway: Evidence from carbon-11 tracer studies.
787 *Plant Science* **188–189**: 97–101.

788 **Griffiths CA, Paul MJ, Foyer CH. 2016.** Metabolite transport and associated sugar signalling systems
789 underpinning source/sink interactions. *Biochimica et Biophysica Acta* **1857**: 1715–1725.

790 **Hafke JB, Van Amerongen JK, Kelling F, Furch ACU, Gaupels F, Van Bel AJE. 2005.** Thermodynamic
791 battle for photosynthate acquisition between sieve tubes and adjoining parenchyma in transport phloem. *Plant*
792 *Physiology* **138**: 1527–1537.

793 **Haritatos E, Ayre BG, Turgeon R. 2000a.** Identification of phloem involved in assimilate loading in leaves by
794 the activity of the galactinol synthase promoter. *Plant Physiology* **123**: 929–937.

795 **Haritatos E, Medville R, Turgeon R. 2000b.** Minor vein structure and sugar transport in *Arabidopsis thaliana*.
796 *Planta* **211**: 105–111.

797 **Hernández-Hernández V, Benítez M, Boudaoud A. 2020.** Interplay between turgor pressure and
798 plasmodesmata during plant development. *Journal of Experimental Botany* **71**: 768–777.

799 **Himmelbach A, Zierold U, Hensel G, Riechen J, Douchkov D, Schweizer P, Kumlehn J. 2007.** A set of
800 modular binary vectors for transformation of cereals. *Plant Physiology* **145**: 1192–1200.

801 **Julius BT, Leach KA, Tran TM, Mertz RA, Braun DM. 2017.** Sugar transporters in plants: New insights and
802 discoveries. *Plant and Cell Physiology* **58**: 1442–1460.

803 **Kim J-Y, Symeonidi E, Pang TY, Denyer T, Weidauer D, Bezruczyk M, Miras M, Zöllner N, Hartwig T,**
804 **Wudick MM, et al. 2021.** Distinct identities of leaf phloem cells revealed by single cell transcriptomics. *The*
805 *Plant Cell* **33**: 511–530.

806 **King RW, Zeevaart JAD. 1974.** Enhancement of phloem exudation from cut petioles by chelating agents. *Plant*
807 *Physiology* **53**: 96–103.

808 **Koch KE. 2004.** Sucrose metabolism: Regulatory mechanisms and pivotal roles in sugar sensing and plant
809 development. *Current Opinion in Plant Biology* **7**: 235–246.

810 **Koncz C, Schell J. 1986.** The promoter of TL-DNA gene 5 controls the tissue-specific expression of chimaeric
811 genes carried by a novel type of *Agrobacterium* binary vector. *MGG Molecular & General Genetics* **204**: 383–
812 396.

813 **Lemoine R, Camera S La, Atanassova R, Dédaldéchamp F, Allario T, Pourtau N, Bonnemain J-L, Laloi**
814 **M, Coutos-Thévenot P, Maurousset L, et al. 2013.** Source-to-sink transport of sugar and regulation by
815 environmental factors. *Frontiers in Plant Science* **4**: 1–21.

816 **Li L, Liu K, Sheen J. 2021.** Dynamic nutrient signaling networks in plants. *Annual Review of Cell and*
817 *Developmental Biology* **37**: 1–27.

818 **Liesche J, Patrick J. 2017.** An update on phloem transport: A simple bulk flow under complex regulation.
819 *F1000Research* **6**: 1–12.

820 **Lohaus G, Pennewiss K, Sattelmacher B, Hussmann M, Muehling KH. 2001.** Is the infiltration-
821 centrifugation technique appropriate for the isolation of apoplastic fluid? A critical evaluation with different
822 plant species. *Physiologia Plantarum* **111**: 457–465.

823 **Lu MZ, Snyder R, Grant J, Tegeder M. 2020.** Manipulation of sucrose phloem and embryo loading affects
824 pea leaf metabolism, carbon and nitrogen partitioning to sinks as well as seed storage pools. *Plant Journal* **101**:
825 217–236.

826 **Martínez-Vilalta J, Sala A, Asensio D, Galiano L, Hoch G, Palacio S, Piper FI, Lloret F. 2016.** Dynamics of
827 non-structural carbohydrates in terrestrial plants: A global synthesis. *Ecological Monographs* **86**: 495–516.

828 **Minchin PEH, Thorpe MR. 1987.** Measurement of unloading and reloading of photo-assimilate within the
829 stem of bean. *Journal of Experimental Botany* **38**: 211–220.

830 **Mustroph A, Zanetti ME, Jang CJH, Holtan HE, Repetti PP, Galbraith DW, Girke T, Bailey-Serres J.**
831 **2009.** Profiling translatoemes of discrete cell populations resolves altered cellular priorities during hypoxia in
832 *Arabidopsis*. *Proceedings of the National Academy of Sciences of the United States of America* **106**: 18843–
833 18848.

834 **Nunes-Nesi A, Fernie AR, Stitt M. 2010.** Metabolic and signaling aspects underpinning the regulation of plant
835 carbon nitrogen interactions. *Molecular Plant* **3**: 973–996.

836 **Ossowski S, Fitz J, Schwab R, Riester M, Detlef W.** <http://wmd3.weigelworld.org>. *personal communication*.

837 **Reiser J, Linka N, Lemke L, Jeblick W, Neuhaus HE. 2004.** Molecular physiological analysis of the two
838 plastidic ATP/ADP transporters from *Arabidopsis*. *Plant Physiology* **136**: 3524–3536.

839 **Rennie EA, Turgeon R. 2009.** A comprehensive picture of phloem loading strategies. *Proc Natl Acad Sci US A*
840 **106**: 14162–14167.

841 **Rosen H. 1957.** A modified ninhydrin colorimetric analysis for amino acids. *Archives of Biochemistry and*
842 *Biophysics* **67**: 10–15.

843 **Ross-Elliott TJ, Jensen KH, Haaning KS, Wager BM, Knoblauch J, Howell AH, Mullendore DL,**
844 **Monteith AG, Paultre D, Yan D, et al. 2017.** Phloem unloading in arabidopsis roots is convective and
845 regulated by the phloem pole pericycle. *eLife* **6**: 1–31.

846 **Sauer N, Stolz J. 1994.** SUC1 and SUC2: two sucrose transporters from *Arabidopsis thaliana*; expression and
847 characterization in baker's yeast and identification of the histidine-tagged protein. *The Plant Journal* **6**: 67–77.

848 **Schulz A. 2015.** Diffusion or bulk flow: how plasmodesmata facilitate pre-phloem transport of assimilates.
849 *Journal of Plant Research* **128**: 49–61.

850 **Sellami S, Le Hir R, Thorpe MR, Vilaine F, Wolff N, Brini F, Dinant S. 2019.** Salinity effects on sugar
851 homeostasis and vascular anatomy in the stem of the *Arabidopsis thaliana* inflorescence. *International Journal*
852 *of Molecular Sciences* **20**: 3167.

853 **Sivitz AB, Reinders A, Ward JM. 2008.** Arabidopsis sucrose transporter AtSUC1 is important for pollen
854 germination and sucrose-induced anthocyanin accumulation. *Plant Physiology* **147**: 92–100.

855 **Solfanelli C, Poggi A, Loreti E, Alpi A, Perata P. 2006.** Sucrose-specific induction of the anthocyanin
856 biosynthetic pathway in Arabidopsis. *Plant Physiology* **140**: 637–646.

857 **Srivastava AC, Dasgupta K, Ajieren E, Costilla G, McGarry RC, Ayre BG. 2009.** Arabidopsis plants
858 harbouring a mutation in *AtSUC2*, encoding the predominant sucrose/proton symporter necessary for efficient
859 phloem transport, are able to complete their life cycle and produce viable seed. *Annals of Botany* **104**: 1121–
860 1128.

861 **Srivastava AC, Ganesan S, Ismail IO, Ayre BG. 2008.** Functional characterization of the Arabidopsis
862 AtSUC2 Sucrose/H⁺ symporter by tissue-specific complementation reveals an essential role in phloem loading
863 but not in long-distance transport. *Plant Physiol* **148**: 200–211.

864 **Stadler R, Sauer N. 1996.** The Arabidopsis thaliana *AtSUC2* gene is specifically expressed in companion cells.
865 *Botanica Acta* **109**: 299–306.

866 **Truernit E, Sauer N. 1995.** The promoter of the *Arabidopsis thaliana* SUC2 sucrose-H⁺ symporter gene directs
867 expression of β -glucuronidase to the phloem: Evidence for phloem loading and unloading by SUC2. *Planta: An*
868 *International Journal of Plant Biology* **196**: 564–570.

869 **Turgeon R. 2006.** Phloem loading: How leaves gain their independence. *BioScience* **56**: 15–24.

870 **Turgeon R. 2010.** The role of phloem loading reconsidered. *Plant Physiology* **152**: 1817–1823.

871 **Turgeon R, Ayre BG. 2005.** Pathways and mechanisms of phloem loading. In: Holbrook NM, Zwieniecki MA,
872 eds. *Vascular Transport in Plants*. Academic press, 45–67.

873 **Vilaine F, Kerchev P, Clement G, Batailler B, Cayla T, Bill L, Gissot L, Dinant S. 2013.** Increased
874 expression of a phloem membrane protein encoded by *NHL26* alters phloem export and sugar partitioning in
875 *Arabidopsis*. *The Plant Cell* **25**: 1689–1708.

876 **Vu DP, Rodrigues CM, Jung B, Meissner G, Klemens PAW, Holtgräwe D, Fürtauer L, Nägele T, Nieberl**
877 **P, Pommerrenig B, et al. 2020.** Vacuolar sucrose homeostasis is critical for plant development, seed properties,
878 and night-time survival in Arabidopsis. *Journal of Experimental Botany* **71**: 4930–4943.

879 **Wippel K, Sauer N. 2012.** Arabidopsis SUC1 loads the phloem in *suc2* mutants when expressed from the *SUC2*
880 promoter. *Journal of Experimental Botany* **63**: 669–679.

881 **Xu Q, Liesche J. 2021.** Sugar export from Arabidopsis leaves: Actors and regulatory strategies. *Journal of*
882 *Experimental Botany* **72**: 5275–5284.

883 **Yan D, Liu Y. 2020.** Diverse regulation of plasmodesmal architecture facilitates adaptation to phloem
884 translocation. *Journal of Experimental Botany* **71**: 2505–2512.
885
886
887
888
889
890
891

Supporting Information

Article title: SUC2 sucrose transporter is required for leaf apoplasmic sucrose levels.
Consequences for phloem loading strategies

Authors: Françoise Vilaine, Laurence Bill, Rozenn Le Hir, Catherine Bellini and Sylvie Dinant

Fig. S1 Characterization of the *NHL*- lines

Fig. S2 Characterization of the *SUC*- lines

Fig. S3 Rate of phloem hexoses and amino acids exudation in *NHL*- and *SUC*- lines

Fig. S4 Fold-changes compared to WT in the exudation rates for sugars and amino acids in *NHL*- and *SUC*- lines

Fig. S5 Phenotype of the *suc1* and *suc2* simple and double mutants

Fig. S6 *In vitro* root growth of WT and *suc2* seedlings in low-sugar medium

Table S1 Primers for genotyping

Table S2 Primers for Gateway^R cloning

Table S3 Vectors for cloning

Table S4 Primers for quantifying genes by RT-qPCR

Table S5 List of genes analyzed by RT-qPCR

Table S6 Correlations (R_{Pearson}) between gene expression and sugar accumulation in rosette leaves

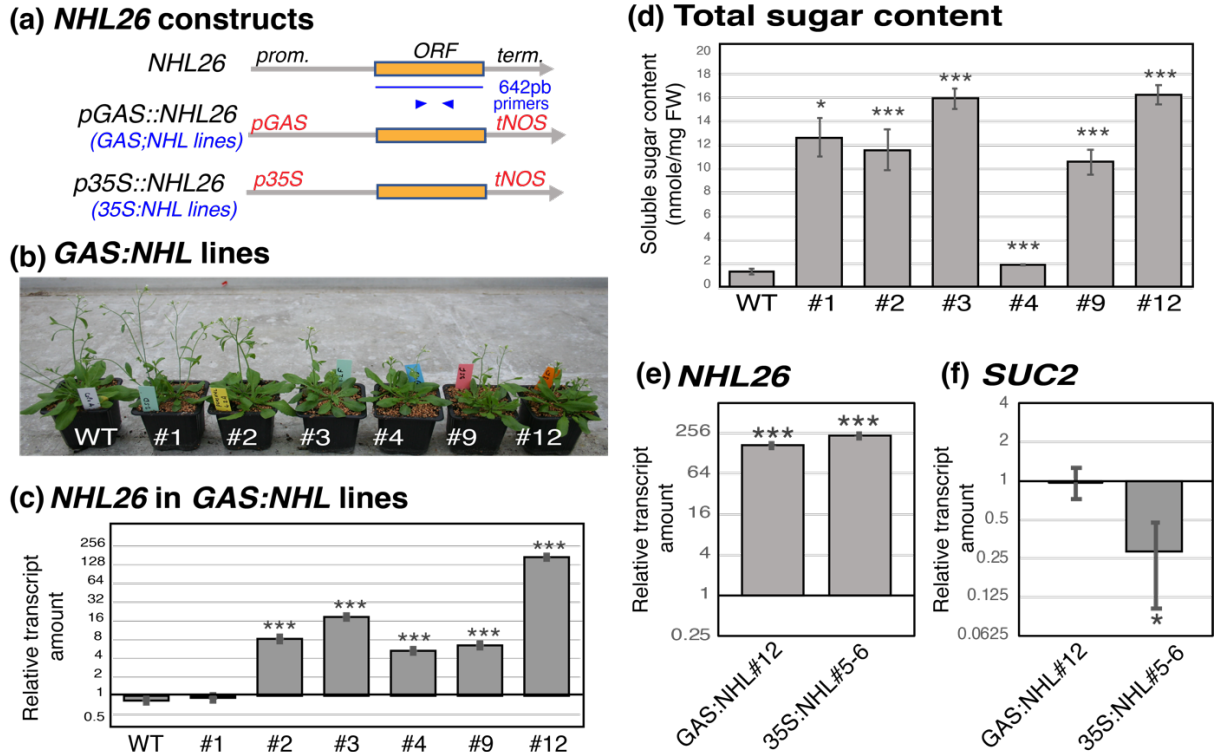


Fig. S1 Characterization of the *NHL*- lines

(a) Schematic representation of *NHL26* constructs. On the top panel: schematic representation of the structure of the *NHL26* gene (AGI number At5g53730). The length of the exon and the position of the primers used for RT-QPCR are indicated below. prom.: promoter, term.: terminator. On the middle panel, representation of the *pGAS::NHL26* construct. The coding region of *NHL26* was fused to the promoter of the *Cucumis melo* galactinol synthase gene to drive gene expression specifically in the minor veins of the mature leaves, as described (Srivastava *et al.*, 2008). On the bottom panel, representation of the *p35S::NHL26* construct (Vilaine *et al.*, 2013). The coding region of *NHL26* was fused to the cauliflower mosaic virus (CaMV) 35S constitutive promoter.

(b) to (f) Phenotypes of 5 weeks-old plants, grown in long-day condition:

(b) Phenotype of representative plants from 6 independent *pGAS::NHL26* transgenic lines (hereafter referred to as *GAS:NHL*).

(c) Relative *NHL26* transcript amount in the *GAS:NHL* transgenic lines. The data are shown on a log₂ scale after normalization by the accumulation of *NHL26* transcripts in WT plants.

(d) Accumulation of total soluble sugars in the *GAS:NHL* transgenic lines. The total sugar contents (glucose, fructose plus sucrose) are expressed in nmoles per mg of fresh weight (FW).

(e) and (f) Relative *NHL26* and *SUC2* transcript amounts in the *GAS:NHL#12* and *p35S::NHL26#5-6* (hereafter referred to as *35S:NHL*) plants. The transcript amount was assessed by qRT-PCR, normalized relative to that of the reference gene *TIP41*, and shown as fold-change compared to wild-type plants, on a log₂ scale. Bar plots and error bars represent the mean and *se* ($n = 6$). Asterisks indicate significant differences compared to control plants (* $p < 0.05$; ** $p < 0.01$; *** $p < 0.001$)

(a) *SUC2* constructs

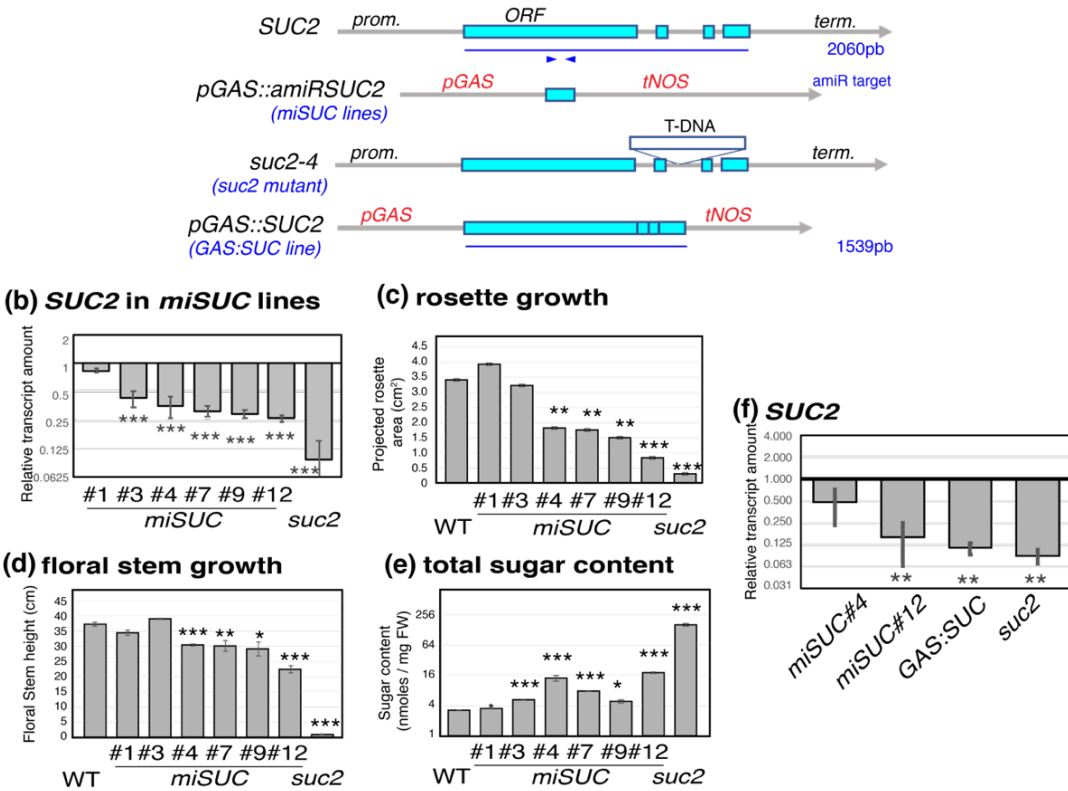


Fig. S2 Characterization of the *SUC*- lines

(a) Schematic representation of *SUC* constructs. On the top panel: schematic representation of the structure of the *SUC2* gene (AGI At1g22710). The length of the coding region (including exons and introns) and the position of the sequence targeted by the *amiRNA* are indicated below. prom.: promoter, term.: terminator. Below, representation of the *pGAS::amiR::SUC2* construct. A microRNA targeting *SUC2* was fused to the promoter of *CmGAS1* to drive microRNA expression specifically in the minor veins of the mature leaves. On the middle panel, representation of the *suc2-4* mutant. On the bottom panel, representation of the *pGAS::SUC2* construct used to partially restore *SUC2* gene in the minor veins of the *suc2-4* mutant.

(b) to (g) phenotypes of plants grown in long-day conditions

(b) Relative *SUC2* transcript amount in representative plants from 6 independent *amiR::SUC2* (hereafter referred to *miSUC*) transgenic lines. The transcript amount was assessed by qRT-PCR, normalized relative to that of the reference gene *TIP41*, and shown as fold-change compared to wild-type plants, on a log₂ scale.

(c) Rosette growth of the representative plants from 6 independent *miSUC* transgenic lines. The projected rosette area was measured at 3 weeks on plants grown in a growth chamber in long-day condition.

(d) Floral stem growth of the representative plants from 6 independent *miSUC* transgenic lines. The height of the floral stem was measured at 5 weeks on plants grown in a growth chamber in long-day condition.

(e) Accumulation of total soluble sugars (glucose, fructose plus sucrose) in representative plants from 6 independent *miSUC* transgenic lines. Sugar contents are expressed in nmoles per mg of fresh weight (FW), shown on a log₂ scale.

(f) Relative *SUC2* transcript amounts in the *miSUC#4*, *miSUC#12*, *suc2pC* and *suc2* plants. The transcript amount was assessed by qRT-PCR, normalized relative to that of the reference gene *TIP41*, and shown as fold-change compared to wild-type plants, on a log₂ scale. Bar plots and error bars represent the mean and *se* (*n* = 6). Asterisks indicate significant differences compared to control plants (* *p* < 0.05; ** *p* < 0.01; *** *p* < 0.001).

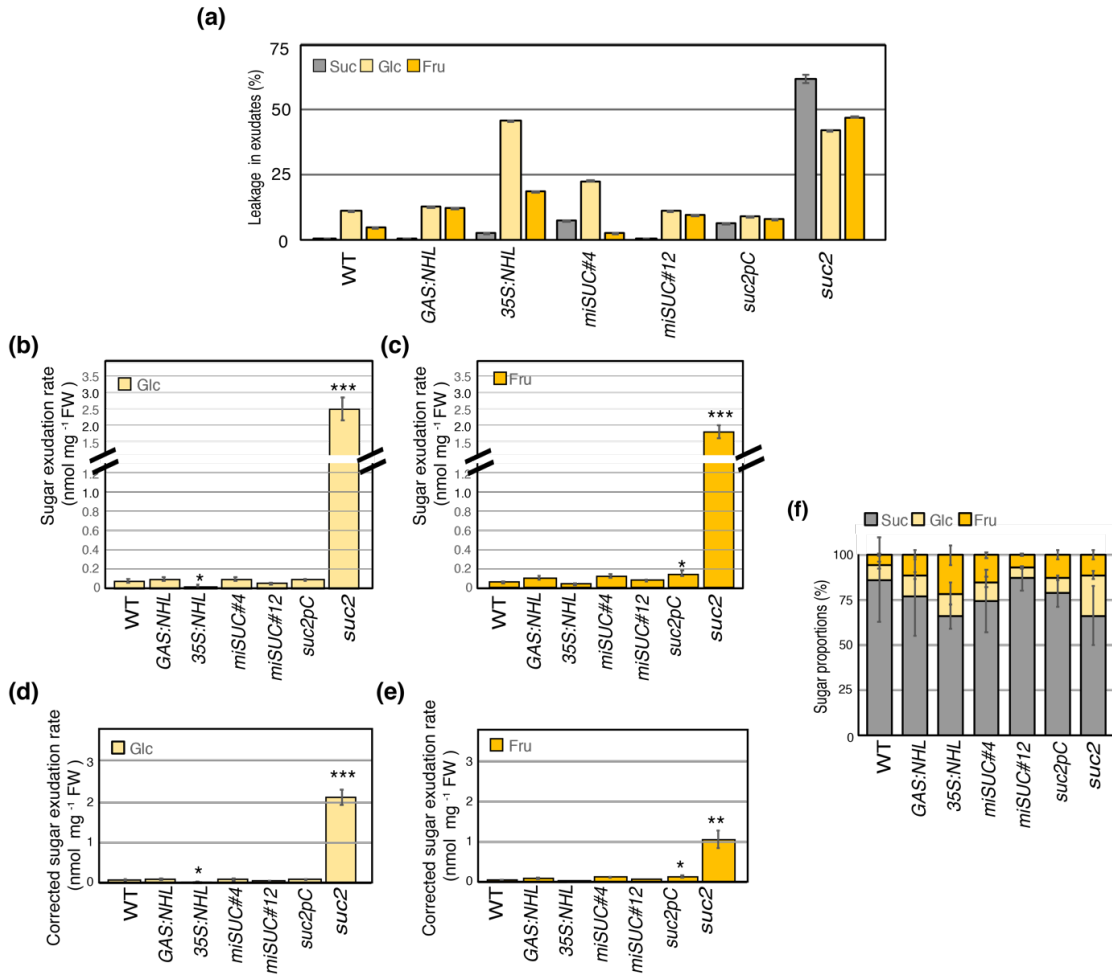


Fig. S3 Rate of phloem hexoses and amino acids exudation in *NHL*- and *SUC*- lines

(a): Sugar leakage was measured on the exudate on a second rosette leaf of the same plant (5th or 6th leaf) collected using the same method but omitting EDTA, for 2 hours of exudation.

(b) and **(c):** Glucose and Fructose exudation rate was measured on the phloem exudate collected by EDTA-facilitated exudation of one rosette leaf per plant (5th or 6th leaf) for 2 hours of exudation.

(d) and **(e):** Corrected Glucose and Fructose exudation rates.

(f): Proportion of disaccharide (sucrose) and monosaccharide (glucose and fructose) in the phloem exudates, after correction for leakage. Bar plots and error bars represent the mean and *se* ($n = 6$). Asterisks indicate significant differences compared to control plants (* $p < 0.05$; ** $p < 0.01$; *** $p < 0.001$). FW: fresh weight.

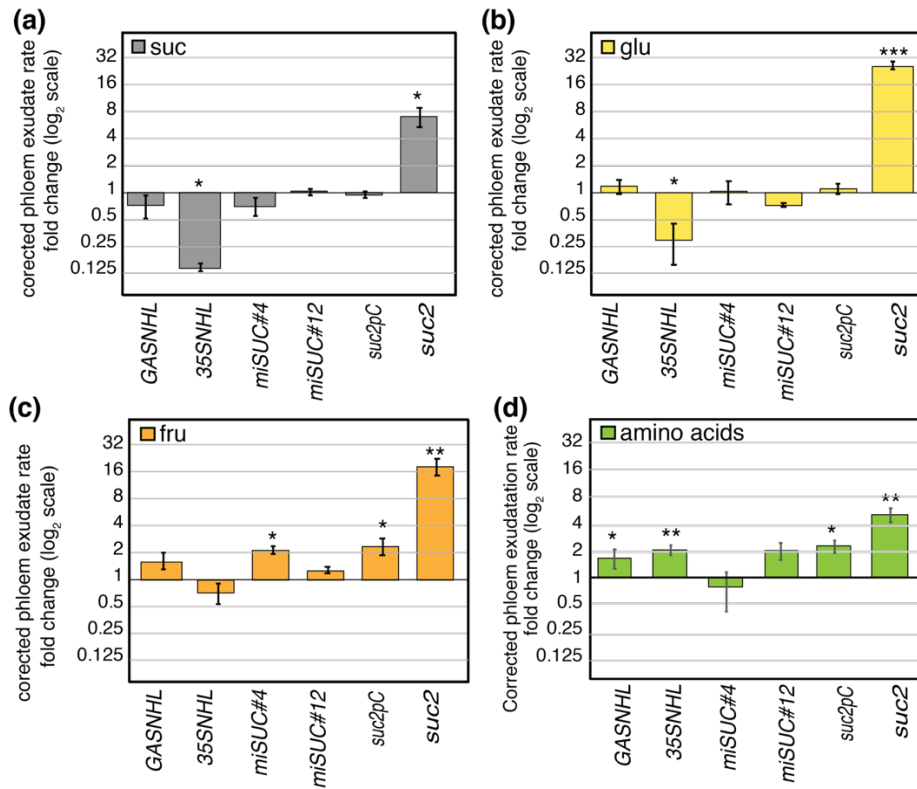


Fig. S4 Fold-changes compared to WT in the exudation rates for sugars and amino acids in *NHL*- and *SUC*- lines

Fold changes compared to WT in the corrected exudation rate of (a) Sucrose, (b) Glucose, (c), Fructose and (d) Total amino acids sugars, calculated by subtracting sugar leakage from the exudation rate of one rosette leaf per plant (5th or 6th leaf). Bar plots and error bars represent the mean and *se* (*n* = 6). Asterisks indicate significant differences compared to control plants (* *p* < 0.05; ** *p* < 0.01; *** *p* < 0.001).

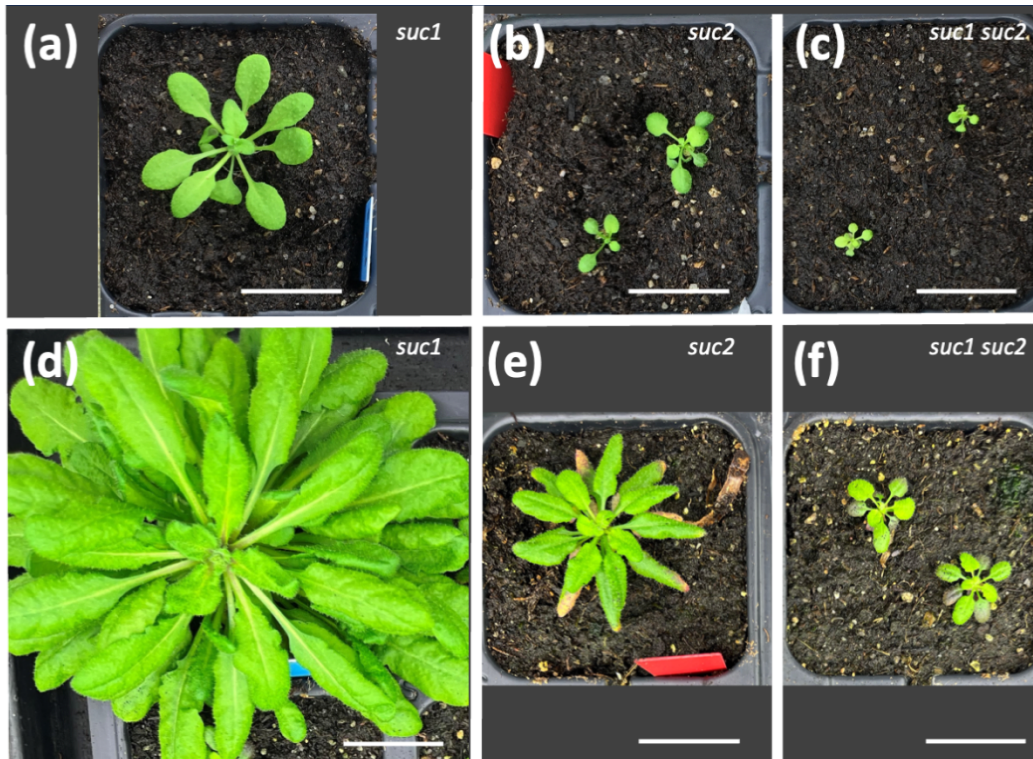


Fig. S5 Phenotype of the *suc1* and *suc2* simple and double mutants

(a) to (c) 8 weeks-old plants; (d) to (f) 12 weeks-old plants, with *suc1* in (a) and (d), *suc2* plants in (b) and (e), and *suc1 suc2* plants on (c) and (f). Plants were grown under short days, to take into account that the plant phenotype tends to be milder for *suc2* when grown under shorter days, as already reported (Srivastava *et al.*, 2009). Bar: 2 cm.

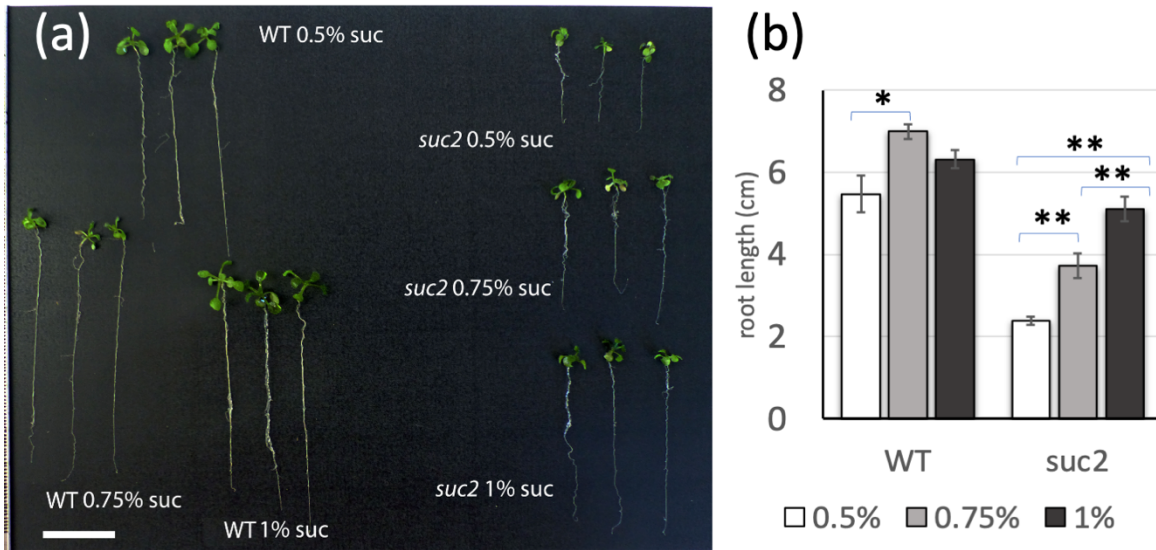


Fig. S6 *In vitro* root growth of WT and *suc2* seedlings

Root growth of WT and *suc2* seedlings grown *in vitro*. **(a)** Plantlets were grown for 15 days on growth medium supplemented with 0.5%, 0.75% or 1% of sucrose (bar = 2 cm). **(b)** Root length ($n=3$ bar: mean \pm SD).

Table S1 Primers for genotyping

Primer	Forward /Reverse	Sequence (5'–3')	Mutant
SUC1-F1101	F	TTCCTTTGTTCCGGTGAAATCTT	Gabi_GK139B11
SUC1-R2113	R	GGTGGTGAAGGTAAAACGGTTA	
GK8474 primer	F	ATAATAACGCTGCGGACATCTACATTTT	
LP-suc2	F	GTTTTTCGGAGAAATCTTCGG	Salk_038124
RP-suc2	R	CAAATGCTGGAATGTTTCCAC	
LBb1.3	F	ATTTTGCCGATTCGGAAC	

Table S2 Primers for Gateway^R cloning

Primer	Forward /Reverse	Sequence (5'–3')	Reference
GWcdsSUC2	F	AAAAAAGCAGGCTATGGTCAGCCATCCAATGGAG	This study
	R	AAGAAAGCTGGGTCAATGAAATCCCATAGTAG	This study
GWcdsNHL26	F	AAAAAAGCAGGCTATGTCTCAAATCTCCATAAC	This study
	R	AAGAAAGCTGGGTTCATATAGTTGTAGAGCAAC	This study
attB1		GGGGACAAGTTTGTACAAAAAAGCAGGCT	(Hartley <i>et al.</i> , 2000)
attB2		GGGGACCACTTTGTACAAGAAAGCTGGGT	(Hartley <i>et al.</i> , 2000)
amiR:SUC2#1		GATAGATCGCATGACTCAGGCATTCTCTTTTTGTATTCC	This study
amiR:SUC2#2		GAATGCCTGAGTCATGCGATCTATCAAAGAGAATCAATGA	This study
amiR:SUC2#3		GAATACCTGAGTCATCCGATCTTTCACAGGTCGTGATATG	This study
amiR:SUC2#4		GAAAGATCGGATGACTCAGGTATCTACATATATATTCCT	This study

Table S3 Vectors for cloning

Plasmids		Reference
pIPK-pGAS-R1R2-tNOS	Gateway binary destination vector, with Galactinol synthase promoter and NOS terminator	This study
pGWB2	Gateway binary destination vector, with CaMV 35S promoter and NOS terminator	(Nakagawa <i>et al.</i> , 2007)
pRS300	Backbone for expressing plant artificial miRNAs	(Schwab <i>et al.</i> , 2006)
pSG3K101	Galactinol synthase promoter	(Haritatos <i>et al.</i> , 2000)
pIPKb001	Gateway destination vector	(Himmelbach <i>et al.</i> , 2007)

Table S4 Primers for quantifying genes by RT-qPCR

Gene	AGI	Forward /Reverse	sequence (5' - 3')	Reference
SUC2	At1g22710	F	TGCCTTTCACGATGACTGAG	(Vilaine <i>et al.</i> , 2013)
		R	TTCCTTGAAAGCTCCGAAGA	
NHL26	At5g53730	F	GTCGGGATCTACTACGACAAGC	This study
		R	CCGTTACGACTGATTTGATAA	
SUC1	At1g71880	F	GGTTCTGGATCCTCGACGTA	This study
		R	CGGAAACATCTTGTGGAGGT	
SWEET2	At3g14770	F	AACAGAGAGTTTAAGACAGAGAGAAG	(Chen <i>et al.</i> , 2010)
		R	ATCCTCCTAAACGTTGGCATTGGT	
SWEET11	At3g48740	F	TCCTTCTCCTAACAACTTATATACCATG	(Chen <i>et al.</i> , 2010)
		R	TCCTATAGAACGTTGGCACAGGA	
SWEET12	At5g23660	F	AAAGCTGATATCTTTCTTACTACTTCGAA	(Chen <i>et al.</i> , 2010)
		R	CTTACAAATCCTATAGAACGTTGGCAC	
SWEET16	At3g16690	F	GAGATGCAAACCTCGGTTCTAGT	(Chen <i>et al.</i> , 2010)
		R	GCACACTTCTCGTCGTCACA	
SWEET17	At4g15920	F	AGTGACAACAAAGAGCGTGAAATAC	(Chen <i>et al.</i> , 2010)
		R	ACTTAAACCGTTGCTTAAACCAACC	
cwINV1	At3g13790	F	CACATGTAAACACATTACATCTCCA	(Sellami <i>et al.</i> , 2019)
		R	TTGGACAATTTTATTGACAACCA	
cwINV3	At1g55120	F	TGTCTTCAACAAAGGCACTCA	(Sellami <i>et al.</i> , 2019)
		R	CGTGACTCTTACGCTCAAT	
cwINV6	At5g11920	F	AGCCCTTGTCCTTCTGAGT	This study
		R	TTCGGCAACAACTGTGACTT	
vINV1	At1g62660	F	TGATTCATCATGTGAGTGAAGAGA	This study
		R	TTGATCGGTGAAAGTGTGGA	
vINV2	At1g12240	F	TGCTCTCTCCCGTACCTGAT	This study
		R	TGATAATGATGTTTCAGTGCCTTT	
cINV1	At1g35580	F	CAATGGTCTTCTCCGTGGT	This study
		R	ACGCACTCGGTACAAAATCC	
cINV2	At4g09510	F	TGGTGTCTTTCGTGGTCAA	(Sellami <i>et al.</i> , 2019)

		R	TATCGGGCTCTCCATTCATC	
PAP1/MYB75	At1g56650	F	AGTTCCTGTAAGAGCTGGGC	This study
		R	GTGCCGTGTTGTAGGAATG	
GSTF12/TT19	At5g17220	F	GGACAGGTAACAGCAGCTTG	This study
		R	ACTTGCCCAAAAGGTTTCGTG	
GPT2	At1g61800	F	CGTAAGGCGGTCAATTCCTA	(Sellami <i>et al.</i> , 2019)
		R	AACGTTAAGTGCCCAACAAG	
RBCS	At5g38410	F	CCGCAACAAGTGGATTCTTGTG	(Vilaine <i>et al.</i> , 2013)
		R	AATGAGCAGAGATAATTCATAAGAATG	
FRK1	At5g51830	F	TCGCTCCTAAAATGCTTCAAA	(Sellami <i>et al.</i> , 2019)
		R	CCGGGAGATCAACAACAAAC	
FRK2	At2g31390	F	CATTCCAGCTCTTCCCTCAG	(Sellami <i>et al.</i> , 2019)
		R	CGATTCAACCATCCGAAAAC	
FRK3	At1g66430	F	CCTTGCTTCAGGACGAAGAG	(Sellami <i>et al.</i> , 2019)
		R	CAGCTTCTTTGGTTGGAAGG	
FRK5	At1g06020	F	TCGTTTGTGGTGCACCTTC	(Sellami <i>et al.</i> , 2019)
		R	AGCTGGAATGGCTCCTTTTT	
FRK6	At1g06030	F	CTTCCATGTTGACGCTGTG	(Sellami <i>et al.</i> , 2019)
		R	CAAGCGTTTGCAAATCTCAG	
FRK7	At3g59480	F	TCAGAGCCTCTGAAAGGAA	(Sellami <i>et al.</i> , 2019)
		R	CCAAAAGCAGGGGAAAATAA	
TPS5	At4g17770	F	TCTGATGCTCCTTCTCCGT	(Bates <i>et al.</i> , 2012)
		R	AGCTGCAAGAGAAGCGAGTC	
APL3	At4g39210	F	CCGGTGTGCTTACGCTATT	This study
		R	ATCAGCTGTGCCTTGAA ACC	
APL4	At2g21590	F	GATTCTTCTTACTCCTTTGCCTTG	This study
		R	CGTGCTTGAACTTTTGATTCC	
TIP41	At4g34270	F	TCCATCAGTCAGAGGCTTCC	(Keech <i>et al.</i> , 2010)
		R	GCTCATCGGTACGCTCTTTT	
TMT1/TST1	At1g20840	F	GAGCTCATCCACATCAGCAA	This study
		R	ATGTTTGGGAATGGGACCGTA	
TMT2/TST2	At4g35300	F	TGCTTCTCACCACGATACCA	(Sellami <i>et al.</i> , 2019)
		R	AACCCATCACGAAGAAGCAG	
ERD16	At1g75220	F	GGAGGCTAGGAATGATTTGC	This study
		R	CGAATTGAATAGGGCCAAGA	
G6PT2	At1g61800	F	CGTAAGGCGGTCAATTCCTA	(Sellami <i>et al.</i> , 2019)
		R	AACGTTAAGTGCCCAACAAG	
STP1	At1g11260	F	TCGTAAAGGAAAAAGTGTATTAGCC	This study
		R	CAATTACAGACAATTAACGAAGAATCA	
STP13	At5g23340	F	CAAGAGGTGGTAAACACACCAA	This study
		R	TCACAAACGCAGTTCAAACCTTA	
LHCB1	At1g29920	F	GGGGTCAGCGGATAGACCAG	(Vilaine <i>et al.</i> , 2013)
		R	CTTTCGCCGAAAGGCTGT	
TRAF1A	At4g00780	F	CTAATCCCGGAACAGCAGAG	This study
		R	TGGTTCCAACGACAAATTCA	This study
RRTF1	At4g34410	F	GTGATCTCAGGGGAAAACGA	This study
		R	GATTTGGCGCGAAAAAGTAG	This study
XIP1	At5g49660	F	CCGGTAGCTTCCCTCTCTCT	This study
		R	ACCATGGAGCATAACGTC	This study

Table S5 List of genes analyzed by RT-qPCR

Function	AGI	Gene	Description
Metabolism			
Starch synthesis	At4g39210	<i>ApL3</i>	ADP-Glucose Pyrophosphorylase Large subunit
	At2g21590	<i>ApL4</i>	ADP-Glucose Pyrophosphorylase Large subunit
Sugar metabolism	At5g51830	<i>FRK1</i>	Fructokinase 1
	At2g31390	<i>FRK2</i>	Fructokinase 2
	At1g66430	<i>FRK3</i>	Fructokinase 3
	At1g06020	<i>FRK5</i>	Fructokinase 5
	At1g06030	<i>FRK6</i>	Fructokinase 6
	At3g59480	<i>FRK7</i>	Fructokinase 7
	At1g35580	<i>cINV1</i>	Cytosolic invertase 1
	At4g09510	<i>cINV2</i>	Cytosolic invertase 2
	At3g13790	<i>cwINV1</i>	Cell wall invertase 1
	At1g55120	<i>cwINV3/6FEH</i>	Fructan exohydrolase /Invertase
	At5g11920	<i>cwINV6/6FEH</i>	Fructan exohydrolase /Invertase
	At1g62660	<i>vINV1</i>	Vacuolar invertase 1
	At1g12240	<i>vINV2</i>	Vacuolar invertase 2
Photosynthesis			
Photosynthesis	At1g29910	<i>LHCB1</i>	Light harvesting CAB binding protein
	At5g38410	<i>RBCS</i>	RuBiSCo small subunit 3b
Signaling			
Glc signaling	At4g29130	<i>HXK1</i>	Hexokinase 1/ GIN2
	At2g19860	<i>HXK2</i>	Hexokinase 2 / sugar sensor
Suc signaling	At4g17770	<i>TPS5</i>	Trehalose synthase 5
NO3 signaling	At5g49660	<i>XIP1</i>	XYLEM INTERMIXED WITH PHLOEM 1 (Peptide receptor like kinase)
ROS signaling	At4g34410	<i>RRTF1</i>	Redox responsive transcription factor 1/ ERF/AP2 family
Stress signaling	At4g00780	<i>TRAF-11</i>	TRAF like (Tumor necrosis factor receptor-associated factor)
Transport			
G6P transporter	At1g61800	<i>G6PT2/GPT2</i>	Glucose6-Phosphate/Phosphate transporter 2
Sugar active transporter	At1g75220	<i>ERD16/ESL1.02</i>	Vacuolar glucose exporter
	At1g11260	<i>STP1</i>	Glucose-proton symporter
	At5g26340	<i>STP13</i>	Hexose-proton symporter
	At1g71880	<i>SUC1</i>	Sucrose-proton symporter 1
	At1g22710	<i>SUC2</i>	Sucrose-proton symporter 2
	At2g02860	<i>SUC3</i>	Sucrose-proton symporter 3
	At1g09960	<i>SUC4</i>	Sucrose-proton symporter 4
At2g14670	<i>SUC8</i>	Sucrose-proton symporter 8	

	At5g06170	<i>SUC9</i>	Sucrose-proton symporter 9
	At1g20840	<i>TMT1/TST1</i>	Tonoplast monosaccharide transporter 1
	At4g35300	<i>TMT2/TST2</i>	Tonoplast monosaccharide transporter 2
Sugar facilitator	At3g48740	<i>SWEET11</i>	Sugar Will Eventually be Exported Transporter 11
	At5g23660	<i>SWEET12</i>	Sugar Will Eventually be Exported Transporter 12
	At3g16690	<i>SWEET16</i>	Sugar Will Eventually be Exported Transporter 16
	At4g15920	<i>SWEET17</i>	Sugar Will Eventually be Exported Transporter 17
	At3g14770	<i>SWEET2</i>	Sugar Will Eventually be Exported Transporter 2
Miscellaneous			
Marker	At4g34270	<i>TIP41</i>	Reference gene
Plasmodesmata	At5g53730	<i>NHL26</i>	Ndr1/Hin1-Like 26, NHL26
Senescence marker	At5g45890	<i>SAG12</i>	Senescence-associated 12
	At4g02380	<i>SAG21</i>	Senescence-associated 21/LEA
Trafficking	At5g17220	<i>GSTF12/TT19</i>	Glutathione S-transferase Phi 12/TT19
Transcription	At1g56650	<i>PAP1/MYB75</i>	Transcription factor MYB75

Table S6 Correlations (R_{Pearson}) between gene expression and sugar accumulation in rosette

leaves

Gene	Correlation	Pval	Gene	Correlation	Pval
<i>SUC1</i>	0.7594	<.0001	<i>cwINV1</i>	0.3872	0.0113
<i>SWEET11</i>	0.7550	<.0001	<i>cwINV6/FEH</i>	0.6925	<.0001
<i>SWEET12</i>	0.7795	<.0001	<i>FRK1</i>	0.6635	<.0001
<i>G6PT2</i>	0.8284	<.0001	<i>FRK2</i>	0.4958	0.0008
<i>APL3</i>	0.7345	<.0001	<i>LHCB1</i>	-0.5347	0.0059

References for Supporting Information

- Bates GW, Rosenthal DM, Sun J, Chattopadhyay M, Peffer E, Yang J, Ort DR, Jones AM. 2012.** A comparative study of the *Arabidopsis thaliana* guard-cell transcriptome and its modulation by sucrose. *PLoS ONE* **7**.
- Chen L-QQ, Hou B-HH, Lalonde S, Takanaga H, Hartung ML, Qu X-QQ, Guo W-JJ, Kim J-GG, Underwood W, Chaudhuri B, et al. 2010.** Sugar transporters for intercellular exchange and nutrition of pathogens. *Nature* **468**: 527–532.
- Haritatos E, Ayre BG, Turgeon R. 2000.** Identification of phloem involved in assimilate loading in leaves by the activity of the galactinol synthase promoter. *Plant Physiology* **123**: 929–937.
- Hartley JL, Temple GF, Brasch MA. 2000.** DNA cloning using in vitro site-specific recombination. *Genome Research* **10**: 1788–1795.
- Himmelbach A, Zierold U, Hensel G, Riechen J, Douchkov D, Schweizer P, Kumlehn J. 2007.** A set of modular binary vectors for transformation of cereals. *Plant Physiology* **145**: 1192–1200.
- Keech O, Pesquet E, Gutierrez L, Ahad A, Bellini C, Smith SM, Gardeström P. 2010.** Leaf senescence is accompanied by an early disruption of the microtubule network in *Arabidopsis*. *Plant Physiology* **154**: 1710–1720.
- Nakagawa T, Kurose T, Hino T, Tanaka K, Kawamukai M, Niwa Y, Toyooka K, Matsuoka K, Jinbo T, Kimura T. 2007.** Development of series of gateway binary vectors, pGWBs, for realizing efficient construction of fusion genes for plant transformation. *Journal of Bioscience and Bioengineering* **104**: 34–41.
- Schwab R, Ossowski S, Riester M, Warthmann N, Weigel D. 2006.** Highly specific gene silencing by artificial microRNAs in *Arabidopsis*. *The Plant cell* **18**: 1121–1133.
- Sellami S, Le Hir R, Thorpe MR, Vilaine F, Wolff N, Brini F, Dinant S. 2019.** Salinity effects on sugar homeostasis and vascular anatomy in the stem of the *Arabidopsis thaliana* inflorescence. *International Journal of Molecular Sciences* **20**: 3167.
- Srivastava AC, Dasgupta K, Ajieren E, Costilla G, McGarry RC, Ayre BG. 2009.** *Arabidopsis* plants harbouring a mutation in *AtSUC2*, encoding the predominant sucrose/proton symporter necessary for efficient phloem transport, are able to complete their life cycle and produce viable seed. *Annals of Botany* **104**: 1121–1128.
- Srivastava AC, Ganesan S, Ismail IO, Ayre BG. 2008.** Functional characterization of the *Arabidopsis* *AtSUC2* Sucrose/H⁺ symporter by tissue-specific complementation reveals an essential role in phloem loading but not in long-distance transport. *Plant Physiol* **148**: 200–211.
- Vilaine F, Kerchev P, Clement G, Batailler B, Cayla T, Bill L, Gissot L, Dinant S. 2013.** Increased expression of a phloem membrane protein encoded by *NHL26* alters phloem export and sugar partitioning in *Arabidopsis*. *The Plant Cell* **25**: 1689–1708.